ID p1

CONTROL HUMAN IPSC-DERIVED ASTROCYTES RESCUE THE DEGENERATIVE PHENOTYPE OF P.A53T-αSYN IPSC-DERIVED NEURONS GENERATED FROM PARKINSON'S DISEASE PATIENTS

O. Apokotou[1], C. Paschou[2], A. Kollias[2], E. Taoufik[2], R. Matsas[2], F. Papastefanaki[1,2]

1. Human Embryonic and Induced Pluripotent Stem Cell Unit, Hellenic Pasteur Institute, Athens, Greece
2. Laboratory of Cellular and Molecular Neurobiology-Stem Cells, Hellenic Pasteur Institute, Athens, Greece

ΕΛΛΗΝΙΚΟ ΙΝΣΤΙΤΟΥΤΟ ΠΑΣΤΕΡ
HELLENIC PASTEUR INSTITUTE

Introduction

Parkinson's disease (PD) is characterized by progressive loss of midbrain dopaminergic neurons resulting in motor and non-motor symptoms. The histopathological disease hallmark is the presence of intraneuronal protein inclusions, termed Lewy bodies and Lewy neurites (1). Approximately 10% of PD cases are associated with mutations in specific genes, such as the p.A53T α-synuclein (αSyn) mutation (G209A in the SNCA gene), causing a familial form of PD with early onset and severe phenotype. While the disease mechanisms remain largely unresolved, cell reprogramming provides a unique human setting for studying PD mechanisms. The aim of our study is to investigate the contribution of non-neuronal cells and their interactions with neurons in PD and uncover novel disease targets for therapy. We have previously established an induced pluripotent stem cell (iPSC)-based neuronal model from patients harboring the p.A53T mutation, which displays disease-associated phenotypes, including protein aggregates, axonal pathology, and compromised network connectivity (2). Here, we generated ventral midbrain-patterned iPSC-derived astrocytes and developed a co-culture system of p.A53T or control neurons on either p.A53T or control astrocytes at all possible combinations, and examined their reciprocal interplay.

References

(1) Desplats P, Lee HJ, Bae EJ, et al. Inclusion formation and neuronal cell death through neuron-to-neuron transmission of alpha-synuclein [published correction appears in Proc Natl Acad Sci USA. 2009 Oct 13;106(41):17606]. Proc Natl Acad Sci USA. 2009;106(31):13010-13015. doi:10.1073/pnas.0903691106

(2) Kouroupi G, Taoufik E, Vlachos IS, et al. Defective synaptic connectivity and axonal neuropathology in a human iPSC-based model of familial Parkinson's disease. Proc Natl Acad Sci USA. 2017;114(18):E3679-E3688. doi:10.1073/pnas.1617259114

Acknowledgements

Funded by the Hellenic Foundation for Research and Innovation (H.F.R.I.) under the "1st Call for H.F.R.I. Research Projects to support Faculty members and Researchers and the procurement of high-cost research equipment" (Project 1019-DiseasePhenoTarget).

H.F.R.I. Hellenic Foundation for Research & Innovation

Methodology

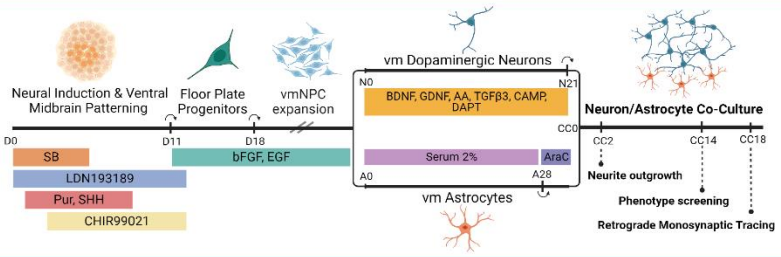

Synaptic Connectivity

LV-TVA-GFP/RV-ENVA-RFP/Nuclei

- Promoted in PD neurons by healthy astrocytes
- Deteriorated in healthy neurons by PD astrocytes

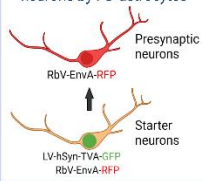

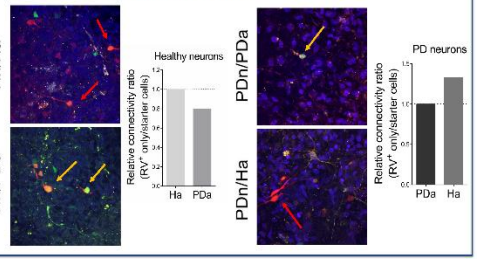

Results

Neurite Outgrowth

- Supported in PD neurons healthy astrocytes
- Compromised in healthy neurons by PD astrocytes

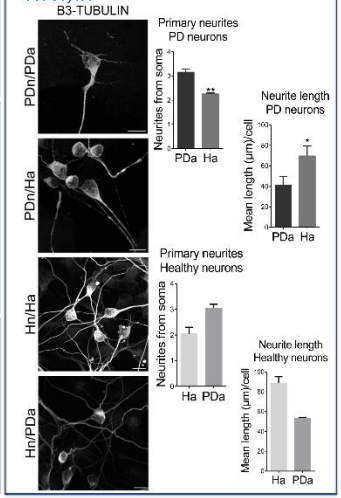

Neuronal Survival

- PD neuronal viability is protected by healthy astrocytes
- Survival of healthy neurons is affected by PD astrocytes

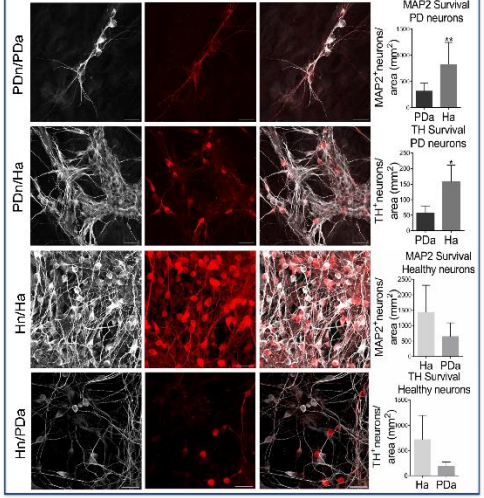

PD-related neuropathology

- Ameliorated in PD neurons by healthy astrocytes
- Aggravated in healthy neurons by PD astrocytes

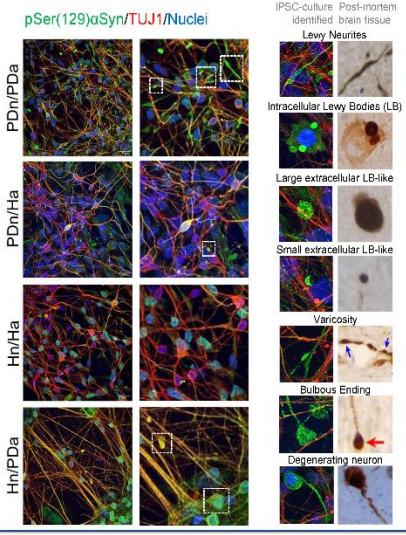

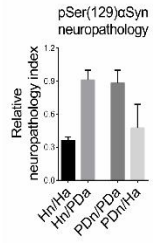

Conclusion

Our data support a critical role of p.A53T astrocytes in the PD associated neurodegeneration process. Furthermore, this study highlights a remarkable ability of healthy astrocytes in rescuing neurodegeneration of p.A53T neurons. The underlying molecular/cellular pathways are being characterized.

ID p2

Investigating the role of the ciliary associated gene-*AHI1* in cortical development using animal models and human brain organoids

Lidia Mouratidou[1,2†], Panagiota Nti Kostantzo[2,3†], Panagiotis Politis[4], Stavros Taraviras[5], Silvia Cappello[6], Christina Kyrousi[1,2]

1. 1st Dep. of Psychiatry, Medical School, NKUA 2. UMHRI (EPIPSI) 3. Athens International Master's Programme in Neurosciences, Dep. of Biology, NKUA 4. BRFAA, 5. Dep. of Physiology, Medical School, University of Patras, 6. Dep. of Developmental Neurobiology, Max Planck Institute of Psychiatry.

INTRODUCTION

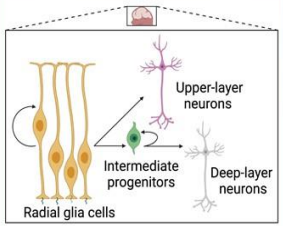

EXPERIMENTAL TIMELINE

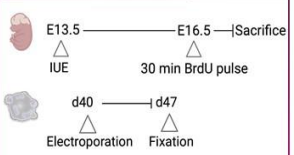

RESULTS

The numbers of progenitors change upon manipulation of *Ahi1*

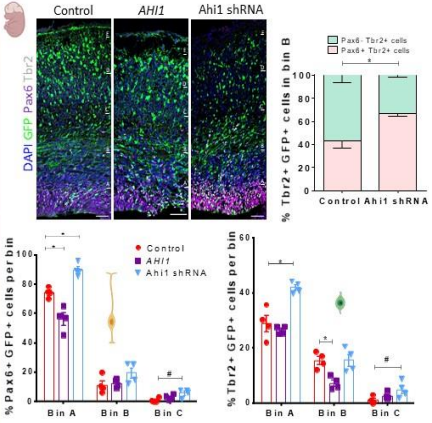

Ahi1 manipulation affects the position of neurons

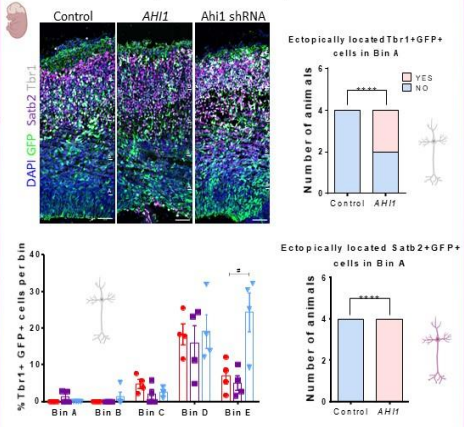

Ahi1 knockdown and overexpression does not change progenitors' proliferation

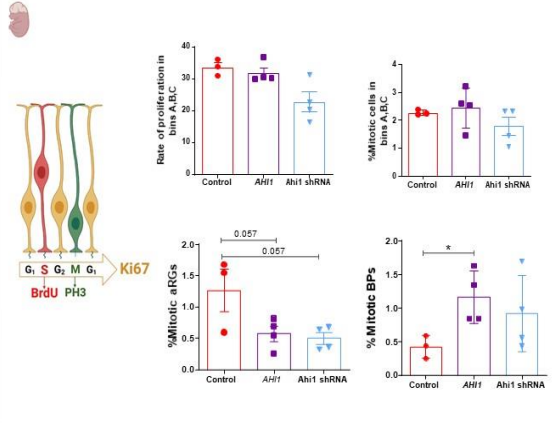

CONCLUSIONS

- Downregulation and overexpression of *Ahi1* affect the numbers and position of apical radial glia cells and intermediate progenitors.
- Manipulation of *Ahi1* leads to the generation of mis specified neural progenitor cells that express both aRGs' and IPs' markers.
- *Ahi1* manipulation alters *the* position of neurons.
- The numbers, length and orientation of primary cilia change upon *Ahi1* manipulation.
- *Ahi1* ectopic expression and downregulation leads to a disrupted apical belt, which is probably the reason behind the altered positioning of progenitors and neurons.
- Manipulation of *Ahi1* changes the ratio between progenitors and neurons in human-derived cerebral organoids, which needs further investigation.

This study was supported by the 2nd Call for H.F.R.I. Research Projects to support Faculty Members and Researchers "The cilium as an organizing center for cortical development and malformations of cortical development".

H.F.R.I. Hellenic Foundation for Research & Innovation

Manipulation of *Ahi1* affect the numbers of progenitors and neurons in human Cerebral organoids

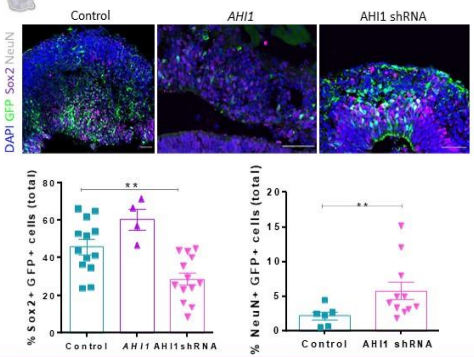

Manipulation of *Ahi1* affects the numbers and length of primary cilia

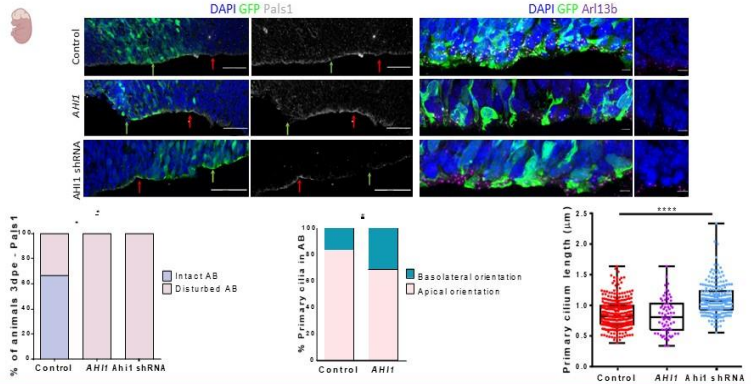

ID p4

Mirk/Dyrk1B kinase controls the generation and the columnar organization of spinal motor neurons via Sonic hedgehog pathway

N. Kokkorakis[1], P.K. Politis[2], V. Nalbadi[1], L. Zagoraiou[2], R. Matsas[1], M. Gaitanou[1]

1. Laboratory of Cellular and Molecular Neurobiology-Stem Cells, Hellenic Pasteur Institute 2. Center of Basic Research, Biomedical Research Foundation of the Academy of Athens

Hellenic Pasteur Institute

Abstract

Objective: Spinal motor neurons (SpMNs) control diverse motor tasks including respiration, posture, and locomotion. SpMNs are organized into median (MMC), lateral (LMC), hypaxial (HMC), and preganglionic (PGC) motor columns respectively. LMC MNs at the brachial and lumbar level of the spinal cord subdivide into medial LMC (LMCm) and lateral LMC (LMCl) columns innervating the muscle limb ventrally and dorsally, respectively. Here, we intend to elucidate the role of the Mirk/Dyrk1B dual-specificity minibrain kinase in the generation, survival, and columnar organization of SpMNs in the developing spinal cord. **Materials and Methods:** We performed *gain-and-loss-of-function* and phenotype rescue studies by applying *in ovo* unilateral electroporation at E2 chick embryonic spinal cord, while the *in vitro* pharmacological inhibition of Dyrk1B kinase activity in E12.5 embryonic mouse primary spinal motor neuron (SpMN) cultures is in progress. **Results:** Functional integration and cross-talk between Mirk/Dyrk1B kinase and Sonic hedgehog/Gli, PI3K/mTOR/AKT, and MEK/ERK signaling pathways affect cellular and molecular processes in development, physiology, and pathology. We revealed a novel role for Mirk/Dyrk1B kinase in the generation of SpMNs in the embryonic chick spinal cord by regulating the Sonic hedgehog (Shh) pathway. Using *in vivo gain-and-loss*-of-function and phenotype rescue approaches in E2 chick spinal cord and its subsequent analysis at E4, we found that Dyrk1B overexpression promoted at E4 cell cycle exit and neuronal differentiation in a cell-autonomous manner, while in a non-cell autonomous manner Dyrk1B overexpression promoted increased apoptosis specifically in the MN domain, followed by a dramatic loss of p2, pMNs, and p3 progenitors, as well as of post-mitotic motor neurons (MNs) and V2a interneurons (INs). This intense ventral phenotype of Dyrk1B overexpression suggested the involvement of Shh signaling. In agreement, real-time RT-qPCR analysis revealed that Dyrk1B overexpression in the E2 chick spinal cord reduces dramatically Shh and Gli3 mRNA levels at E4. At E6, the loss of MNs is selectively reflected in reduced LMCm MNs that innervate the muscle limbs ventrally. In phenotype rescue experiments, the compromised Shh signaling, due to Dyrk1B overexpression, was restored by using AZ191 compound, a specific Dyrk1B kinase inhibitor, or SAG agonist of Smoothened (SMO), which activates the Shh pathway. Both compounds resulted in the restoration of p2, pMNs, and p3 progenitors, as well as of LMCm MNs. The specific effect of Dyrk1B in LMCm MNs could be explained by our finding that Shh is expressed exclusively by LMCm MNs at the E6 chick spinal cord. Pharmacological inhibition of Dyrk1B kinase activity in E12.5 mouse MNs primary cultures is in progress. Conclusions: In conclusion, Mirk/Dyrk1B kinase acts as a transcriptional suppressor of the Sonic hedgehog pathway, thus regulating the number of p2, pMNs, and p3 progenitors that are under the strong influence of Shh gradient, and especially controls the generation and survival of SpMNs as well as their columnar organization in the LMCm column.

Results

1. Dyrk1B is expressed by cycling neuronal progenitors in the VZ and by post-mitotic motor neurons (MNs) in the MZ of chick and mouse spinal cord respectively.

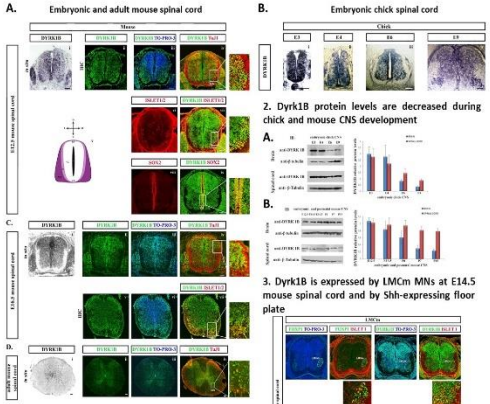

2. Dyrk1B protein levels are decreased during chick and mouse *CNS* development

3. Dyrk1B is expressed by LMCm MNs at E14.5 mouse spinal cord and by Shh-expressing floor plate

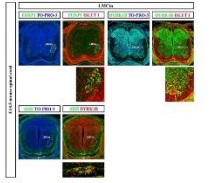

4. Dyrk1B overexpression at E2 promoted at E4 cell cycle exit and neuronal differentiation in a cell-autonomous manner

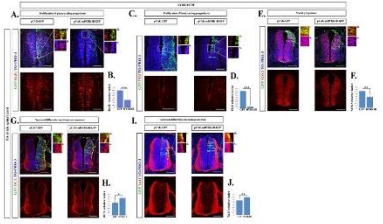

5. Overexpression of Dyrk1B at E2 chick spinal cord promoted at E4 premature cell cycle exit combined with increased apoptosis in ventral spinal cord and MN domain in a non-cell autonomous manner resulting in the reduction of the total number of motor neuron progenitors (pMNs), post-mitotic MNs, as well as V2a INs.

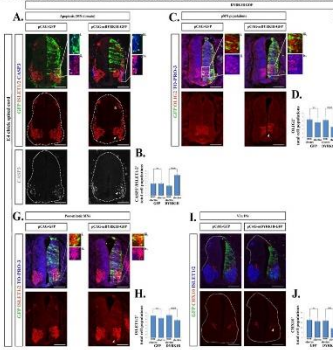

6. *In vivo gain-and-loss-of-function and mechanistic phenotype rescue* experiments at E2 chick spinal cord showed at E4 that AZ191 reversed the strong effect of Dyrk1B on cell cycle exit by increasing the total number of proliferating PH3$^+$cells (A,B) and of post-mitotic MNs (C,D).

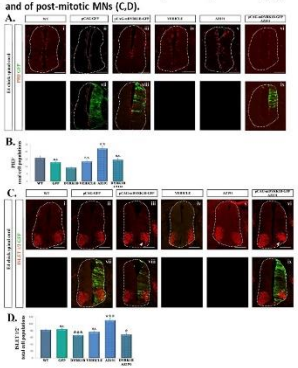

7. Dyrk1B overexpression at E2 reduced dramatically at E4, Shh and Gli3 mRNA levels (A,B), while Dyrk1B inactivation by using AZ191 (D) or Shh activation by using SAG (E,F) increased the mRNA expression of Shh (C,D,E) and Gli3 (C) suggesting that Dyrk1B is a potent transcriptional suppressor of Shh and Gli3.

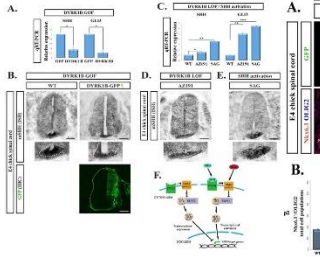

8. In *gain-of-function* experiments (GOF), Dyrk1B overexpression at E2 promoted at E4, in a non-cell autonomous manner, dramatic loss of p2, pMNs, and p3 progenitors. In *loss-of-function* experiments (LOF), the inhibition of Dyrk1B by using AZ191 or the activation of Shh by using SAG promoted increased number of p2, pMN, and p3 progenitors. In rescue phenotype experiments by using AZ191 or SAG, the progenitor populations were restored (A-D).

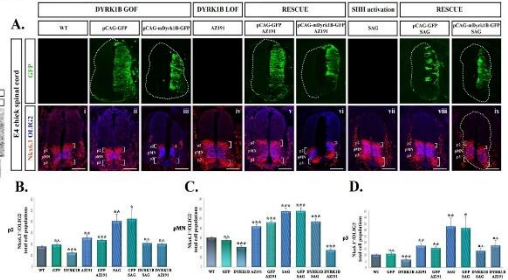

9. The observed loss of MNs at E4, as a consequence of Dyrk1B overexpression at E2, is selectively reflected at E6 in reduced LMCm MN population (A, B). Notably, LMCm MNs innervate the muscle limbs ventrally (C). In *loss-of-function (LOF)* experiments by using AZ191 the LMCm motor column was increased (D, E), as the same effect was observed when we activated Shh pathway by using SAG (F, G), thus indicating that Shh regulates LMCm MN formation.

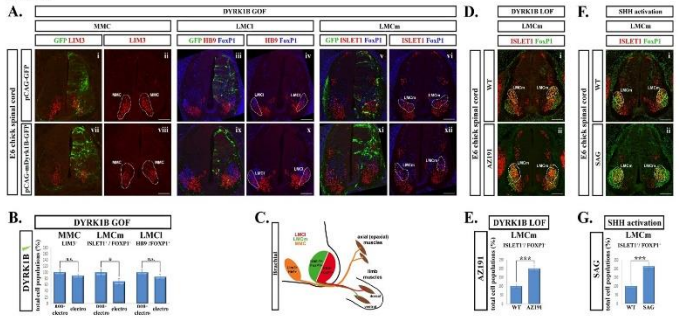

10. Notably, Shh is expressed exclusively by LMCm MNs at E6 (E), while Dyrk1B is expressed in whole MN domain (E).

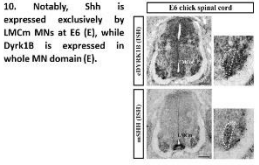

11. Our study suggests that Dyrk1B acts as an upstream transcriptional suppressor of Shh and Gli3, during spinal cord development regulating the generation and survival of SpMNs as well as their columnar organization.

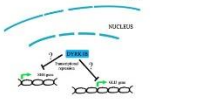

Conclusion: Dyrk1B acts as a potent upsteam transcriptional suppressor of Shh and Gli3, during spinal cord development, thus regulating the number of all progenitor populations that are under the strong influence of Shh gradient, and especially controls the generation and survival of SpMNs as well as their columnar organization.

ID p5

Evaluation of induction of fetal hemoglobin synthesis by genome editing of *cis*- and *trans*-acting components of the β-globin locus

*Panayiota L. Papasavva[1], Nikoletta Y. Papaioannou[1], Lola Koniali[1], Basma Naiisseh[1], Soteroula Christou[4], Maria Sitarou[4], Michael N. Antoniou[5], Toni Cathomen[2,3], Marina Kleanthous[1,‡], Carsten W. Lederer[1,‡], * Petros Patsali[1,‡]*

(1) Department of Molecular Genetics Thalassemia, The Cyprus Institute of Neurology and Genetics, Nicosia 2371, Cyprus, (2) Institute for Transfusion Medicine and Gene Therapy, Medical Center – University of Freiburg, Freiburg, Germany (3) Center for Chronic Immunodeficiency, Medical Center – University of Freiburg, Freiburg, Germany (4) Thalassemia Clinics, Cyprus Ministry of Health, Cyprus (5) Department of Medical and Molecular Genetics, King's College London, London, United Kingdom, ‡Contributed equally to this work ,*Corresponding author: Carsten W. Lederer, email: lederer@cing.ac.cy

BACKGROUND & AIM

Reactivation of γ-globin can ameliorate the clinical phenotype of β-hemoglobinopathies by functional compensation of β-globin deficiency and anti-sickling action of fetal hemoglobin (HbF). It is thus a universal therapy approach, potentially applicable to all β-hemoglobinopathy patients, irrespective of genotype.[1]

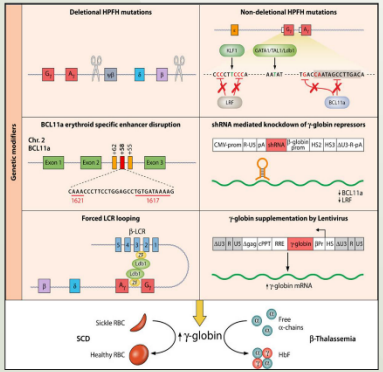

Figure 1 Therapeutic approaches based on γ-globin expression. Reproduced from[1]

MATERIALS & METHODS

We explored genetic modification of globin expression regulators and the β-globin locus as potential therapeutic approaches for β-hemoglobinopathies by reactivation of γ-globin. To this end, we employed the CRISPR/Cas9 system to abolish expression of two known γ-globin repressors, BCL11A, by targeting its erythroid enhancer, and ZBTB7A (trans editing), and a dual-targeting single RNA-guided CRISPR/Cas12a system to create a large (7.4-kb) β-δ intergenic deletion at the β-globin locus (cis editing) (Figure 2). Tools were delivered as ribonucleoprotein (RNP) complexes by nucleofection in HUDEP-2 and primary thalassemic CD34+ cells. Edited cells were assessed for on-target editing efficiency by Inference of CRISPR Edits (ICE)3 and digital polymerase chain reaction (dPCR), and analysed after erythroid differentiation by HPLC for globin/hemoglobin expression and by flow cytometry for intracellular HbF expression. Analysis of clonal populations of HUDEP-2 cells bearing the 7.4-kb deletion is underway to confirm findings in bulk edited cell populations.

RESULTS

1. Deletion mutations in the β-globin gene cluster

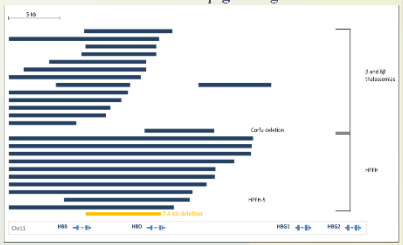

Figure 2 Large HBB locus deletions. Schematic diagram of known large genomic deletions (>7 kb) in the β-globin cluster causing thalassemia or hereditary persistence of fetal hemoglobin (HPFH) (blue bars). The large 7.4-kb deletion created by our dual-targeting single RNA-guided CRISPR/Cas12a system is indicated by the yellow bar. Modified from[2]

2. Analysis of editing efficiency

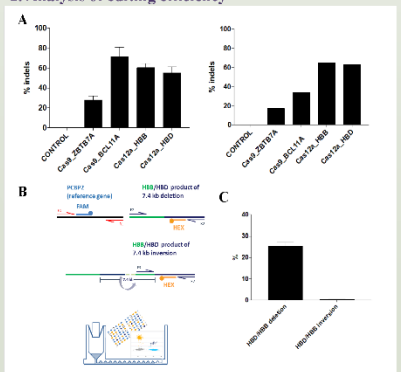

Figure 3 Editing efficiency. (A) Assessment of on-target indel mutations created by CRISPR/Cas9 and CRISPR/Cas12a systems at ZBTB7A, BCL11A, HBB and HBD loci in nucleofected HUDEP-2 (n=4) (left) and primary thalassemic CD34+ cells (n=1) (right) by ICE[3] (B) Schematic of the nanoplate-based dPCR duplex assay developed to detect the 7.4-kb deletion or inversion in Cas12a_HBB/HBD edited HUDEP-2 cells. The PCBP2 gene was used as a reference gene. (C) Quantification of the HBB/HBD 7.4-kb deletion and inversion in Cas12a_HBB/HBD edited HUDEP-2 cells (n=4). Error bars represent the SD.

3. HPLC quantification of globins and hemoglobins

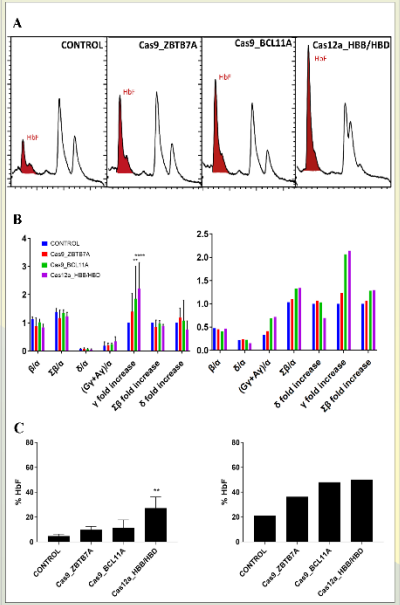

Figure 4 HPLC analyses of HUDEP-2 and primary thalassemic CD34+ cells across treatments. (A) Chromatograms of hemoglobin expression in patient-derived thalassemic CD34+ cells. (B) Analysis of globin expression in HUDEP-2 cells (n=4) (left chart) and patient-derived thalassemic CD34+ cells (n=1) (right chart) (mean + standard error of the mean (SEM)), ****P=0.0001, **P=0.0038 (vs. CONTROL). (C) Percentages of HbF expression in HUDEP-2 cells (n=4) (left chart) and patient-derived thalassemic CD34+ cells (n=1) (right chart) (mean = SEM), **P=0.0025 (vs. CONTROL).

RESULTS

4. Flow cytometry analysis of HbF epression

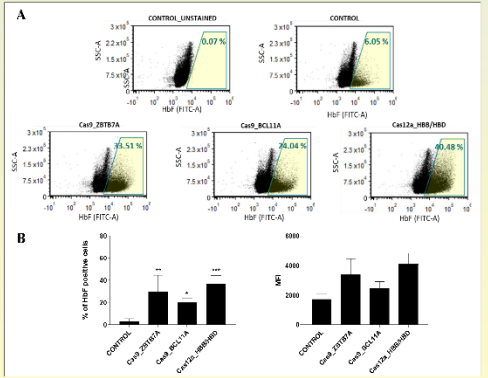

Figure 5 Flow cytometry analysis of HbF positive cells (A) Representative flow cytometric analysis plots of differentiated HUDEP-2 cells stained with anti-HbF antibody. CONTROL_UNSTAINED serves as negative control. (B) Percentages of HbF positive cells and (C) mean fluorescence intensity (MFI) in HUDEP-2 cells (n=4). Error bars represent the SD. *P=0.0447, **P=0.0028, ***P=0.0004 (vs. CONTROL).

CONCLUSIONS

Preliminary results of the study suggest that generation of the 7.4-kb cis deletion at the β-locus, relying on the highly efficient non-homologous end-joining (NHEJ) repair mechanism of double-strand breaks (DSBs), may lead to higher HbF levels than the disruption of key trans-acting components and γ-globin repressors BCL11A and ZBTB7A, which are also involved in other essential functions of hematopoiesis

REFERENCES

1. Srinivasan S, Babu P, Thangavel S (2020) Manipulation of Developmental Gamma-Globin Gene Expression: an Approach for Healing Hemoglobinopathies. Mol Cell Biol 41:1. 2. Antoniani C, Meneghini V, Lattanzi A, Felix T, Romano O, Magrin E, Weber L, Pavani G, Hoss S El, Kurita R, et al (2018) Induction of fetal hemoglobin synthesis by CRISPR/Cas9-mediated editing of the human β-globin locus. Blood 131:1960–1973. 3. Conant D, Hsiau T, Rossi N, Oki J, Maures T, Waite K, Yang J, Joshi S, Kelso R, Holden K, et al (2022) Inference of CRISPR Edits from Sanger Trace Data. Crispr J 5:123–130.

The project "New Infrastructure for the Diagnosis and Therapy of Patients" is funded by the Norway Grants 2014-2021. The projects EXCELLENCE/1216/0092 and EXCELLENCE/0421/0086 are co-financed by the European Regional Development Fund and the Republic of Cyprus through the Research and Innovation Foundation. Additional funding was received through TELETHON and Eurobank PhD studentships for the Cyprus Institute of Neurology and Genetics.

ID p6

CELL-INTRINSIC PATHOLOGICAL CHARACTERISTICS IN A53T-ASYN IPSC-DERIVED ASTROCYTES FROM PARKINSON'S DISEASE PATIENTS

ΕΛΛΗΝΙΚΟ ΙΝΣΤΙΤΟΥΤΟ ΠΑΣΤΕΡ
INSTITUT PASTEUR HELLENIQUE

C. Paschou[1], A. Kollias[1], K. Charmpi[1], O. Apokotou[2], P. Handris[1], M. Samiotaki[3], G. Panayotou[3], E. Taoufik[1], R. Matsas[1], F. Papastefanaki[1, 2]

[1] Laboratory of Cellular and Molecular Neurobiology-Stem Cells, Hellenic Pasteur Institute, Athens, Greece [2] Human Embryonic and Induced Pluripotent Stem Cell Unit, Hellenic Pasteur Institute, Athens, Greece [3] Institute of Bioinnovation, Biomedical Sciences Research Center "Alexander Fleming", Vari, 16672, Greece.

Introduction

Astrocytes, the most abundant cells in the human brain play critical roles in neuronal health while they can exert neuroprotective or neurotoxic effects upon disease. However, their involvement in Parkinson's disease (PD) has only recently started being appreciated. Accumulating evidence suggesting astrocytes as important players in neuronal dysfunction and interplays between astrocytes and neurons may provide insights into PD pathology. **Here we used our previously established human induced pluripotent stem cell (iPSC) model[1] to investigate if the endogenous expression of pA53T-αSyn, an autosomal dominant mutation of alpha-Synuclein related with PD, in astrocytes causes cell-autonomous dysfunction.**

Materials and Methods

Characterization of ventral midbrain-patterned astrocytes derived from healthy and pA53T-αSyn iPSCs (iAstro) was performed on day 28 of differentiation. Treatments with proinflammatory cytokines TNFα, IL-1α and C1q (TIC) or Thapsigargin (Tg) were assessed after day 44. Quantification of p(Ser129)αSyn puncta and protein aggregates was performed using the FIJI macro "AggreCount".

Immunofluorescence Confocal | Real Time RT PCR | Proteomic Analysis

REFERENCES

1. Kouroupi G, Taoufik E, Vlachos IS, Tsioras K, Antoniou N, Papastefanaki F, Chroni-Tzartou D, Wrasidlo W, Bohl D, Stellas D, Politis PK, Vekrellis K, Papadimitriou D, Stefanis L, Bregestovski P, Hatzigeorgiou AG, Masliah E, Matsas R. Defective synaptic connectivity and axonal neuropathology in a human iPSC-based model of familial Parkinson's disease. Proc Natl Acad Sci U S A. 2017 May 2;114(18):E3679-E3688. doi 10.1073/pnas.1617259114. Epub 2017 Apr 17. PMID: 28416701; PMCID: PMC5422768.

ΕΛ.Ι.Δ.Ε.Κ. Ελληνικό Ίδρυμα Έρευνας & Καινοτομίας

ACKNOWLEDGMENT: This work is funded by the Hellenic Foundation for Research and Innovation (H.F.R.I.) under the "1st Call for H.F.R.I. Research Projects to support Faculty members and Researchers and the procurement of high-cost research equipment" (Project 1019-DiseasePhenoTarget).

Successful generation of iAstrocytes

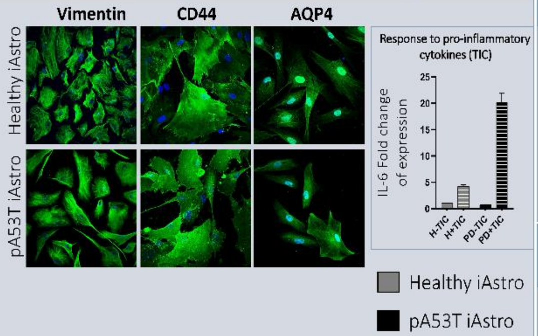

pA53T iAstro display higher levels of αSyn, with increased aggregates of p(Ser129)αSyn

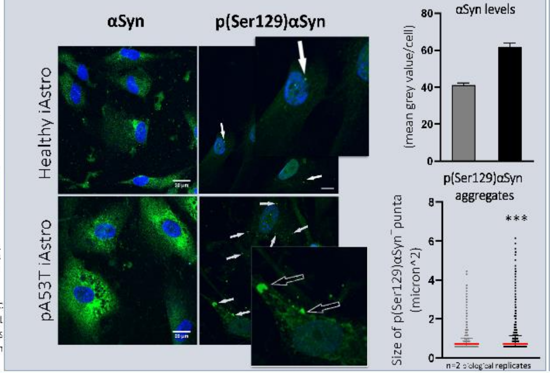

pA53T iAstro display cytoplasmic vacualization and aberrant calcium transients

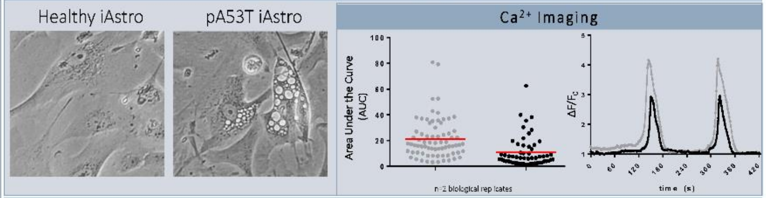

Pathological features of pA53T iAstro related to protein quality control and degradation systems

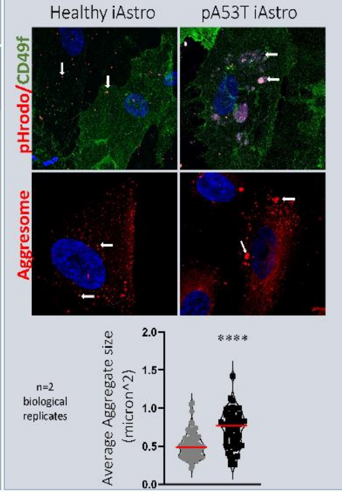

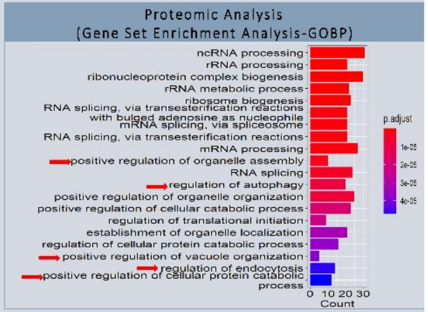
Proteomic Analysis
(Gene Set Enrichment Analysis-GOBP)
ncRNA processing
rRNA processing
ribonucleoprotein complex biogenesis
rRNA metabolic process
ribosome biogenesis
RNA splicing, via transesterification reactions with bulged adenosine as nucleophile
mRNA splicing, via spliceosome
RNA splicing, via transesterification reactions
mRNA processing
positive regulation of organelle assembly
RNA splicing
regulation of autophagy
positive regulation of organelle organization
positive regulation of cellular catabolic process
regulation of translational initiation
establishment of organelle localization
regulation of cellular protein catabolic process
positive regulation of vacuole organization
regulation of endocytosis
positive regulation of cellular protein catabolic process
Count
p.adjust

ER Stress-related Unfolded Protein Response

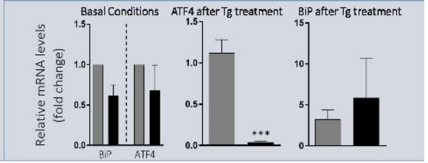

Conclusion: Our data demonstrate that the p.A53T-αSyn mutation causes intrinsic dysregulation in astrocytes, related with proteostasis and clearance mechanisms that may have a critical contribution in PD neuropathology.

ID p7

IN VIVO MICROGLIAL BIN1 DELETION FOLLOWING LPS-INDUCED NEUROINFLAMMATION REGULATES MICROGLIA PROLIFERATION AND INFLAMMATORY RESPONSE

M. Margariti[1], E. Papadimitriou[1], I. Thanou[1], A. Pelletier[2], M.A. Roussaki[1], E. Xingi[3], M. Avloniti[5], V. Kyrargiri[5], M. Costa[2,4], D. Thomaidou[1]

[1] Hellenic Pasteur Institute, Neural Stem Cells and Neuro-imaging Group, Department of Neurobiology, Athens, Greece, [2] Institut Pasteur de Lille, Univ. Lille, Inserm, CHU Lille, Lille, France, [3] Hellenic Pasteur Institute, Light Microscopy Unit, Athens, Greece, [4] Federal University of Rio Grande do Norte, Brain Institute, Natal, Brazil, [5] Hellenic Pasteur Institute, Laboratory of Molecular Genetics, Microbiology Department, Athens, Greece

Introduction

Microglial activation has been recently considered a crucial player in the pathogenesis of the majority of neurodegenerative diseases including AD. However, the contribution of microglia activation in AD progression has been controversial. Genome-Wide Association Studies have identified several Single Nucleotide Polymorphisms (SNPs) strongly associated to increased risk of developing Late Onset Alzheimer's Disease (LOAD), many of which are related to microglia activation. SNPs in the locus harboring Bridging Integrator 1 (BIN1) gene show the strongest association with AD, after Apolipoprotein E. BIN1 is a member of the Bin/Amphiphysin/Rvs (BAR) family of adaptor proteins implicated in cell membrane modelling dynamics. Although, its role in neurons has been studied both in vitro and in vivo, the role of BIN1 in microglial activation state and its contribution in LOAD pathology remains to be clarified. To this end we have developed a conditional transgenic Cx3CR1 Cre-ERT2//Bin1 fl/fl mouse, in which BIN1 is knocked-out in microglial cells upon tamoxifen administration. Furthermore, we have challenged BIN1-KO mice with LPS, to investigate the effect of microglia-specific Bin1 deletion on mouse brain under homeostatic and inflammatory conditions. We are analyzing the transcriptomic profile of all brain cell populations by snRNA-Seq to reveal novel targets related to microglial BIN1 and we are performing real time PCR and immunohistochemical analysis to validate our sequencing data.

Creation of inducible microglial BIN-KO mouse model

Tamoxifen and LPS administration protocol

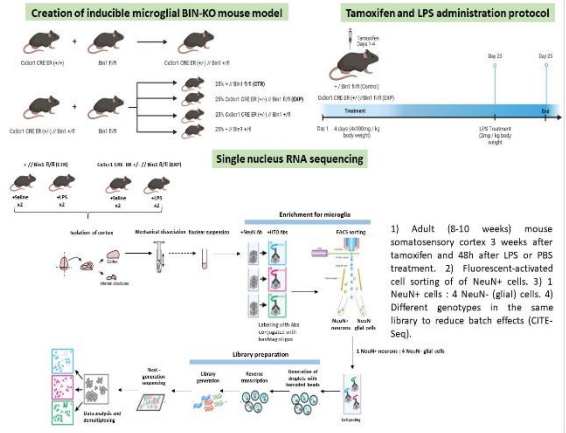

1) Adult (8-10 weeks) mouse somatosensory cortex 3 weeks after tamoxifen and 48h after LPS or PBS treatment. 2) Fluorescent-activated cell sorting of NeuN+ cells. 3) 1 NeuN+ cells : 4 NeuN- (glial) cells. 4) Different genotypes in the same library to reduce batch effects (CITE-Seq).

Bin1 is efficiently knocked out in microglial cell population

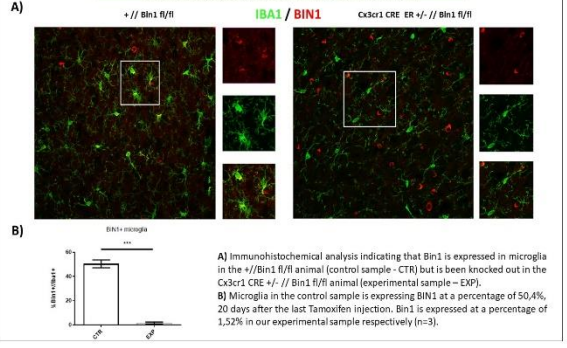

A) Immunohistochemical analysis indicating that Bin1 is expressed in microglia in the +//Bin1 fl/fl animal (control sample - CTR) but is been knocked out in the Cx3cr1 CRE +/- // Bin1 fl/fl animal (experimental sample – EXP).
B) Microglia in the control sample is expressing BIN1 at a percentage of 50,4%, 20 days after the last Tamoxifen injection. Bin1 is expressed at a percentage of 1,52% in our experimental sample respectively (n=3).

Identification of microglial subpopulations after BIN1 KO and LPS treatment in the mouse brain

Seurat analysis

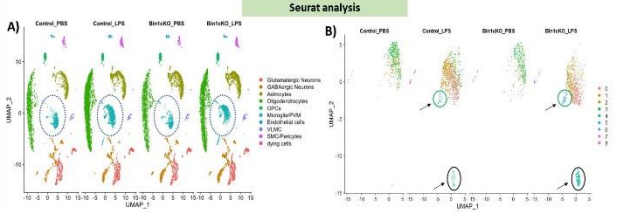

A) Analysis of cell populations from the sn-RNA seq. The map is showing all the different populations that arose. The microglial population (circled) was analyzed further.
B) Identification of 9 microglial subpopulations. Two distinct microglial subpopulations (4, black circles and 6, green circles) are more abundant following LPS treatment and get further increased in BIN1 KO.

Scenic analysis

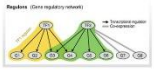

SCENIC software was used for the discovery of different microglial cell subpopulations / states based on expression of TFs and cis-regulatory sequences in the sc-RNA-Seq data.

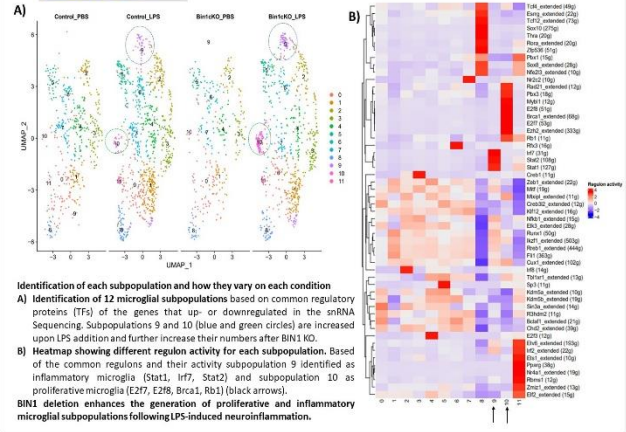

Identification of each subpopulation and how they vary on each condition

A) Identification of 12 microglial subpopulations based on common regulatory proteins (TFs) of the genes that up- or downregulated in the snRNA Sequencing. Subpopulations 9 and 10 (blue and green circles) are increased upon LPS addition and further increase their numbers after BIN1 KO.
B) Heatmap showing different regulon activity for each subpopulation. Based of the common regulons and their activity subpopulation 9 identified as inflammatory microglia (Stat1, Irf7, Stat2) and subpopulation 10 as proliferative microglia (E2f7, E2f8, Brca1, Rb1) (black arrows).
BIN1 deletion enhances the generation of proliferative and inflammatory microglial subpopulations following LPS-induced neuroinflammation.

Increased microglial proliferation in the brain of microglia – specific BIN1 KO mice both in resting and LPS-activated microglia (after LPS treatment)

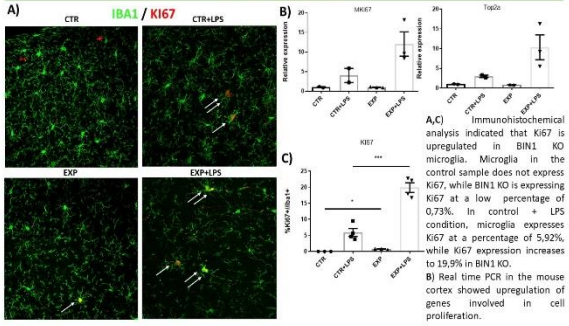

A,C) Immunohistochemical analysis indicated that Ki67 is upregulated in BIN1 KO microglia. Microglia in the control sample does not express Ki67, while BIN1 KO is expressing Ki67 at a low percentage of 0,73%. In control + LPS condition, microglia expresses Ki67 at a percentage of 5,92%, while Ki67 expression increases to 19,9% in BIN1 KO.
B) Real time PCR in the mouse cortex showed upregulation of genes involved in cell proliferation.

Upregulation of pro-inflammatory genes after microglial BIN1 KO and LPS treatment

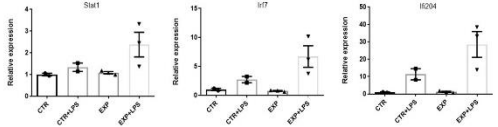

Real time PCR in the mouse cortex indicated upregulation of pro-inflammatory genes and genes involved in IFN-type I - mediated inflammatory response in BIN1 KO under LPS-induced inflammation.

Conclusions

- Establishment of an inducible microglial BIN1 KO mouse model and performance of sn-RNA seq analysis
- Identification of two different microglial subpopulations enhanced after LPS treatment and further increased in BIN1 KO model
- BIN1 regulates microglia proliferation and IFN-type I - mediated inflammatory response in the mouse adult brain after LPS treatment.

Funding

Supported by Institut Pasteur Network *PTR-MIAD Program (2020-2022)* and *Nostos Foundation fellowship* to M. Margariti *(2023-2026)*.

ID p8

EFFICIENT EPIGENETICALLY-MEDIATED REACTIVATION OF GAMMA GLOBIN EXPRESSION IN AN IMMORTALIZED HUMAN ERYTHROID PROGENITOR CELL LINE

Fotios Papadopoulos[1,2] , Kiriaki Paschoudi [1,2] , Agapi Pantou[1,2,] , Theodora Intzou[1,2] ,Evangelia Yannaki[1,2,3] , Nikoleta Psatha[1]

[1]*Department of Genetics, Development and Molecular Biology, School of Biology, Aristotle University of Thessaloniki, Greece,*

[2]*Gene and Cell Therapy Center, Hematology-HCT Unit, G. Papanikolaou Hospital, Thessaloniki, Greece,*

[3]*Division of Hematology, Department of Medicine, University of Washington, Seattle, WA, USA*

INTRODUCTION

Over the last few years, the development of genome editing approaches for beta-hemoglobinopathies enabled the targeted introduction of genomic tools to either correct point mutations or induce disease-modifying mutations, such as the reactivation of gamma globin to cure β-hemoglobinopathies. Despite the promising results that have emerged from clinical and preclinical genome editing applications, limitations still exist due to the generation of potentially harmful off- and on- target effects, related to the induction of double strand brakes(DSB). Recently, the development of custom-designed epigenome editors (epi-editors) has enabled the development of alternative and less invasive approaches for targeted gene regulation. Aim of the present study is to address the feasibility and the efficacy of epigenetically mediating gamma globin

EXPERIMENTAL DESIGN

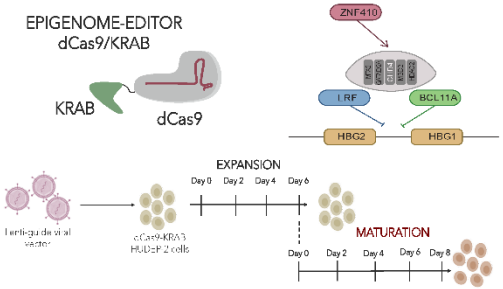

First, we established a HUDEP-2 cell line that stably expressed the epigenome editor-dCas9-KRAB (dCas9/KRAB HUDEP-2 cells). Next, we designed gRNAs that target cis-regulatory elements of the three master regulators of gamma globin expression during development, BCL11A, ZNF410, LRF. Following transduction with lenti-guide vectors, dCas9/KRAB HUDEP-2 cells were cultured both in expansion and maturation medium.

RESULTS

In order to introduce specific epigenetic alterations, we used the gRNAs depicted below to target specifically the erythroid enhancer of BCL11A, along with the ZBTB7A and the recently identified HBG-suppressor, ZNF410 promoters.

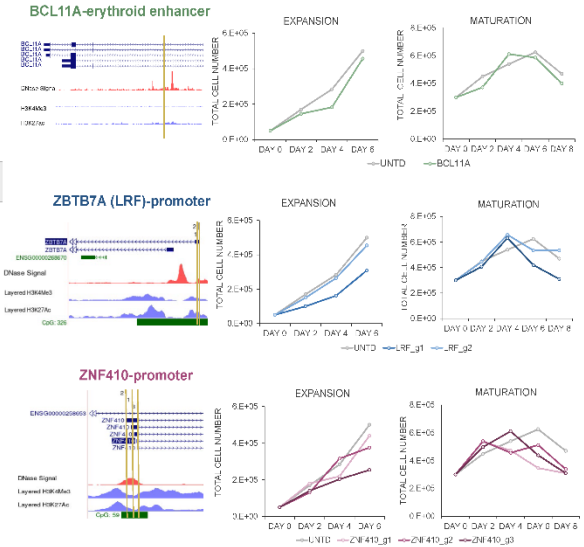

Epigenetic suppression was generally well tolerated and didn't affect cell proliferation during expansion or maturation. We did however observe a small reduction in cell numbers by targeting LRF promoter with LRF_g2.

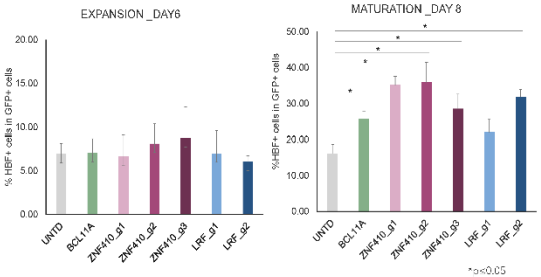

During expansion we didn't observe significant differences in HbF levels. However, at later stages of maturation we noticed a significant increase of %HbF+ cells within the transduced populations in all groups. This HbF increase was significantly pronounced when targeting the ZNF410 promoter compared to both the BCL11a-enhancer and ZBTB7A-promoter.

CONCLUSIONS

Overall, the epigenetic mediated inactivation of the three gamma globin master regulators, BCL11A, LRF, ZNF410, seems to be feasible and effective, leading to significant HbF induction in HUDEP-2 cells during maturation. Future studies in primary cells are required to explore translatability of these results.

References

1. Yannaki E, et al. *Hum Gene Ther.* 2021
2. Fontana, L , et. al *Genes* 2023.
3. Thakore PI, et. al. *Nat Methods.* 2015

Funding

H.F.R.I. Hellenic Foundation for Research & Innovation

EHA Advanced Research Grant

ID p9

ΕΛΛΗΝΙΚΟ ΙΝΣΤΙΤΟΥΤΟ ΠΑΣΤΕΡ
INSTITUT PASTEUR HELLENIQUE

Disrupted neurogenesis and increased neuroinflammation following brain chemical lesion

Mirka Fourmouzi 1 *, Eleni Makarouni 1 *, Irini Thanou 1 , Mary Margariti 1, Dimitra Thomaidou1

1 Department of Neurobiology, Hellenic Pasteur Institute, 127 Vas. Sofias Avenue, 11521 Athens, Greece
*equal contribution

INTRODUCTION

Long-term adverse side effects of chemotherapy, also known as "Chemo-Brain", have been only recently anticipated and several mechanisms are proposed to be involved in changes regarding brain structure and function following systematic use of chemotherapeutic agents. These include reduction of Neural Stem Cell (NSC) proliferation rates in adult brain neurogenic zones, white matter degeneration and inflammation. This phenomenon is particularly pronounced in cancers, such as glioblastoma, which are inherently resistant to chemotherapy requiring high doses of chemotherapy to eliminate them, resulting in its high concentration in the cerebrospinal fluid. Aim of the project is to investigate the response of adult brain's subgranular zone of dentate gyrus of the hippocampus to widely used antimitotic/ chemotherapeutic agents.

PROTOCOL

In order to investigate the response of adult brain's neurogenic zones and, as well as, adjacent brain parenchyma areas, to widely used antimitotic/ chemotherapeutic agents, the agent Cytosine Arabinoside (**Ara-C**) is administered in two stereotaxic intraventricular injections (single dose 0,3 mg/kg).

RESULTS

1 Dynamic changes in the population of DCX+ cells in the DG niche.

❑ Loss of dendritic projections and abnormal migration of DCX+ cells deeper into the GCL.

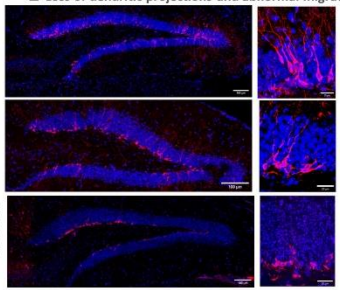

1. A disorientation of dendritic projections of DCX+ cells into the GCL is observed 15 days after the Ara-C infusion. However, no difference is observed in the number of DCX+ neuroblasts between Ara-C and control conditions. DCX (red). Scale bar 100μm.

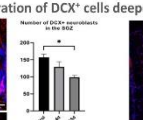

2. Quantification of number of DCX+ cells in SGZ on Ara-C and control conditions. p= 0,88. Ara-c n=2, Ctl n=2.

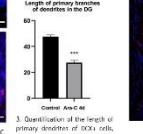

3. Quantification of the length of primary dendrites of DCX+ cells, located in the SGZ of the hippocampus, on control and Ara-C treated mice(4d). Ctl n=5, Ara-C 4d n=3.

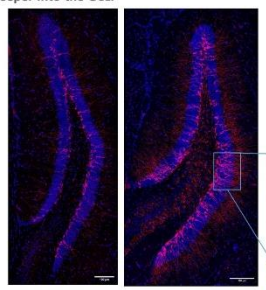

4. Immunostaining for DCX on control and Ara-C treated mice (6 weeks)I in the DG of hippocampus. DCX (red), DAPI (blue). Coronal sections 20μm. Scale bar 100μm.

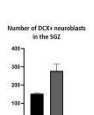

5. Quantification of the number of DCX+ cells in SGZ on Ara-C and control conditions. Ara-c n=4, Ctl n=2.

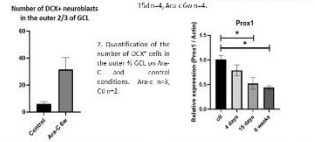

6. Representative image of DCX+ neuroblasts abnormally migrated into the outer GCL (Granule Cell Layer). The drawn line defines the boundaries between SGZ and GCL. Coronal sections 20um. Scale bar 100μm.

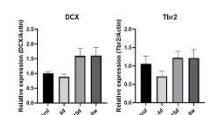

7. Temporal fluctuations in the expression of neuroblasts markers, DCX and Tbr2, with a transient decrease followed by an increase at 6 weeks. Ctr n=4, Ara-C 4d n=4, Ara-C 15d n=4, Ara-C 6w n=4.

8. Steady decrease of immature granule cells marker Prox1. P=0,0222, P=0,0087. Ctr n=4, Ara-c 4d n=4, Ara-c 15d n=3, Ara-c 6w n=3.

2 Disrupted neuronal lineage progression in DG.

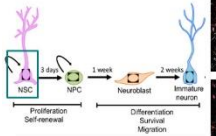

1. Representative image of the morphology of the GFAP, Sox2 double positive cells that were quantified.

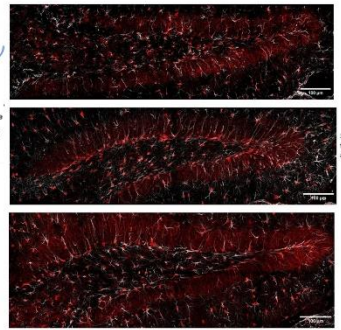

7. Immunostaining for GFAP and Sox2 in the DG of the hippocampus on control and Ara-C treated mice (4d and 15d). GFAP (white), Sox2 (red). Sagittal Sections 20 μm. Scale bar 100μm.

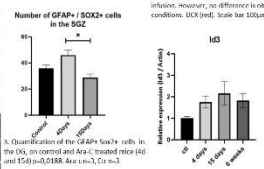

5. Quantification of the GFAP+ Sox2+ cells in the DG, on control and Ara-C treated mice (4d and 15d) p=0,0188. Ara-c n=3, Ctr n=3

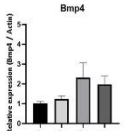

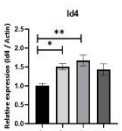

4.Transient increase of Id4, Id3 and Bmp4 expression 15 days post infusion followed by decrease at 6 weeks. P=0,0295, P=0,0048. Ctr n=4, Ara-c 4d n=4, Ara-c 15d n=4, Ara-c 6w n=4.

3 Persistent astro- and micro-gliosis in the DG

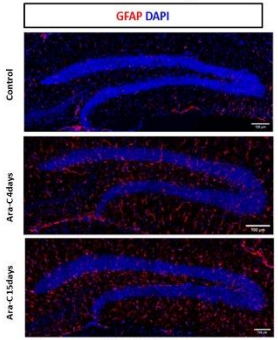

1. Immunostaining for GFAP in the DG of the hippocampus on control and Ara-C treated mice (4d and 15d). GFAP (red), DAPI (blue). Sagittal Sections 20 μm. Scale bar 100μm.

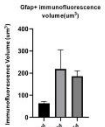

2. Quantification of the GFAP+ cells volume in the DG, on control and Ara-C treated mice (4d and 15d).

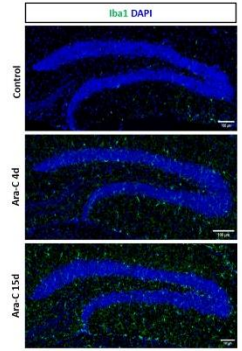

3. Immunostaining for Iba1 in the DG of the hippocampus on control and Ara-C treated mice (4d and 15d). Iba1(green), DAPI (blue). Sagittal Sections 20 μm. Scale bar 100μm.

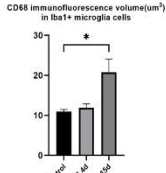

4. Quantification of the CD68 volume in Iba1+ cells in the DG, on control and Ara-C treated mice (4d and 15d). Ctl vs Ara-c 15d * p<0,05. Ctl n=3, Ara-C 4d n=3, Ara-C 15d n=2.

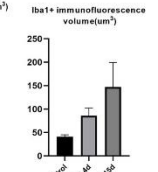

5. Quantification of the Iba1+ cells volume in the DG, on control and Ara-C treated mice (4d and 15d).

CONCLUSIONS

- Ara-C intraventricular (IV) injection results in altered cell dynamics in the SGZ of the DG of hippocampus, indicated by a statistical significant decrease of the DCX+ cells at 4 and 15 days accompanied by a transient increase of the NSCs with radial morphology specifically at 4 days. The decrease in DCX+ neuroblasts is completely overturned at 6 weeks where a notable augmentation of DCX+ neuroblasts as compared to control condition is evident.
- The loss of dendritic projections of DCX+ neuroblasts along with the abnormal migration deeper into the granule cell layer following Ara-C administration, may be indicative of neuroblasts disturbed or delayed maturation.
- The increased numbers of NSCs at 4 days post Ara-C administration is supported by the elevated expression of the quiescent transcription factor Bmp4 and each downstream target Id4, both controlling NSCs quiescence.

- Further, Ara-C triggers neuroinflammation in both adult neurogenic niches and adjacent regions, with an extensive presence of reactive astroglia and microglia.
- Our studies are on-going to further investigate the molecular profile of the niche and quantify the differences in hippocampal neurogenesis at different time points following Ara-C administration.

Supported by Greek Ministry of Education (MIS 5002480) - Invest by the Operational Programme "Competitiveness, Entrepreneurship and Innovation" (NSRF 2014-2020) and co-financed by Greece and the European Union (European Regional Development Fund). Stavros Niarchos Foundation Grant.
All imaging and image analysis took place in the Light Microscopy Unit of the Hellenic Pasteur Institute.

ID p10

PML REGULATES THE SPECIFICATION AND POTENTIATES THE SURVIVAL OF NEURAL STEM CELLS

Sirago Spanou[1,2], Takis Makatounakis[1], Joseph Papamatheakis[2], Androniki Kretsovali[1]*

[1] *IMBB, FORTH, Heraklion, Greece,* [2] *Biology Department, University of Crete, Heraklion, Greece*

**Corresponding author: Androniki Kretsovali, email: kretsova@imbb.forth.gr*

INTRODUCTION & AIM OF STUDY

The Promyelocytic Leukemia Protein (PML) originally characterized as a tumor suppressor, regulates various biological processes, such as gene transcription, cell proliferation and apoptosis. In embryonic (ESCs) and induced pluripotent (iPSCs) stem cells PML is required for maintenance of the naïve and acquisition of the induced pluripotency state. Recent studies report PML as a hub gene for Alzheimer's Disease (AD) and that PML bodies co-localize with the c'-terminal region of Amyloid Precursor Protein (APP-CT) in correlation with AD pathophysiology. Although previous studies suggest that PML regulates neuronal plasticity and clearance of toxic poly-Q protein aggregates, there is no conclusive evidence for a role in neuroprotection or neurodegeneration. **In this work we examine the role of PML in neuronal cell specification and survival from neurotoxic stress. We also study the involvement of PML in AD employing the 5xFAD mouse model.**

RESULTS & DISCUSSION

eNSC survival following β-amyloid stress

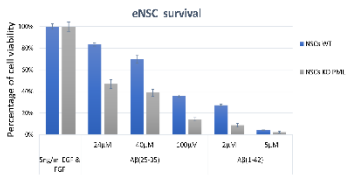

PML KO eNSC are more vulnerable to β-amyloid stress than the WT. eNSC survival was determined by MTT assay. Cells were exposed to β-amyloids for 48 hours.

PML acts via the PI3K/pAkt/mTOR and STAT-3 signaling pathways

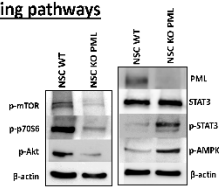

In the absence of PML, activated levels of mTOR, p-70s6 kinase and Akt are decreased, whereas activated levels of STAT3 and AMPK are increased.

PML protects eNSC from apoptotic death and potentiates the autophagic flux

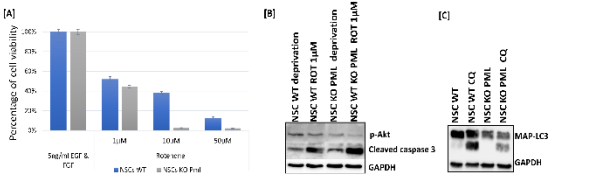

[A] PML KO eNSC are vulnerable to rotenone (mitochondria electron transport blocker). eNSC survival determined by MTT assay. **[B]** Increased protein expression of cleaved-caspase 3 upon rotenone treatment. **[C]** Protein expression of MAP-LC3II is decreased in the absence of PML in eNSC upon chloroquine treatment (autophagy inhibitor).

PML influences the choice between neuronal vs astrocyte differentiation of eNSC

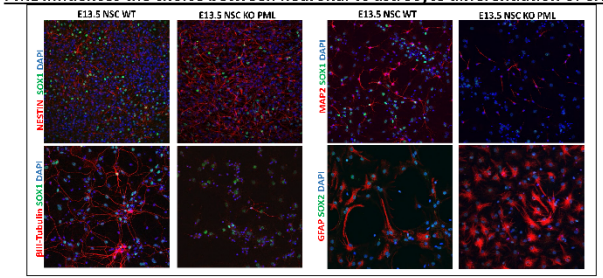

Immunofluorescence for MAP2,βIII-Tubulin and GFAP in differentiated eNSC, 9DIV (x40). Absence of PML resulted in fewer MAP2/βIII-Tubulin neuron generation and promoted astrocyte differentiation.

Reduced nuclear expression of PML in 5xFAD mice compared to the WT

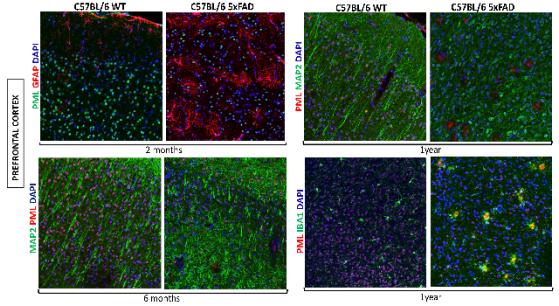

Immunohistochemistry for PML, GFAP, MAP2 and IBA-1 from 2, 6 months and 1 year old C57BL/6 WT and C57BL/6 5xFAD prefrontal cortex sections (x40). PML is not expressed in GFAP positive astrocytes. PML is expressed in MAP2 positive neurons.

PML regulates mitochondrial respiration and ROS production in eNSC in eNSC

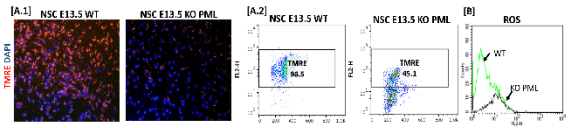

[A.1] In the absence PML, the mitochondrial membrane potential is highly decreased, as seen in reduced TMRE staining. **[A.2], [B]** Flow cytometry analysis (FACS) in eNSC stained for TMRE and MitoSOX revealed decreased mitochondrial membrane potential and increased ROS production in KO PML eNSC.

We propose that PML:

- **is required for neuronal specification of eNSC.**
- **shows a neuroprotective function *in vitro* by enhancing the defence against β-amyloid and apoptotic stress, sustaining the mitochondrial integrity and potentiating the autophagic flux of neuronal cells.**
- **might exert a neuroprotective function *in vivo*.**

This research is co-financed by **"DINNESMIN-MIS 5032840"** and IMBB-FORTH internal funding.

ID p11

DEVELOPMENT OF MECHANO-ACTIVE SCAFFOLDS FOR ENHANCED OSTEOGENIC DIFFERENTIATION

Nikoleta Natalia Tavernaraki [1], Varvara Platania [1], Maria Chatzinikolaidou [1,2]

[1] Department of Materials Science and Technology, University of Crete, Heraklion, Greece
[2] Institute of Electronic Structure and Laser, Foundation for Research and Technology Hellas (FORTH), Greece

6th Congress of the Hellenic Society of Gene Therapy and Regenerative Medicine
May 26-28, 2023
Cotsen Hall, American School of Classical Studies Athens

Purpose of the study

Bone is a highly dynamic tissue that undergoes continuous mechanical forces through lifetime. Mechanical stimuli applied on scaffolds resembling the human bone tissue have major effect on osteogenesis [1]. Poly(3,4-ethylenedioxythiophene, PEDOT) is a piezoelectric polymer that responds to mechanical stimulation producing an electrical signal that promotes the osteogenic differentiation of pre-osteoblastic cells by opening voltage-gated calcium channels [2]. The aim of this study is to examine the biocompatibility and osteogenic responses of pre-osteoblastic cells cultured onto novel tissue engineered piezoelectric PEDOT-containing scaffolds applying mechanical stimulation.

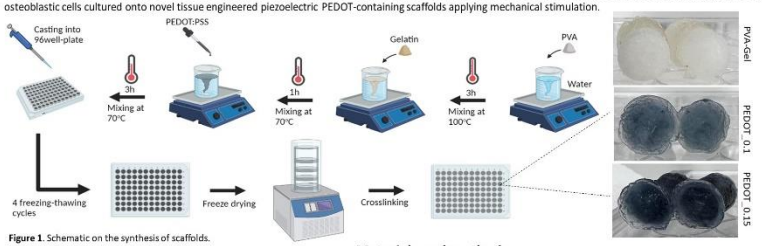

Figure 1. Schematic on the synthesis of scaffolds.

Materials and methods

Two different concentrations of PEDOT (0.15% w/v and 0.10% w/v) were combined with a 5% w/v poly(vinyl alcohol) (PVA) and 5% w/v gelatin, casted into wells , freeze dried and crosslinked with 2% v/v (3-glycidyloxypropyl)trimethoxy silane (GOPS) and 0.025% w/v glutaraldehyde. Non-crosslinked scaffolds for all compositions were also evaluated for comparison. Crosslinked (C) and non-crosslinked scaffolds without PEDOT were employed as control. Physicochemical characterization was performed by means of the % porosity, swelling and degradation rates and FTIR analysis. All scaffolds compositions were mechanically characterized by measuring their Young's modulus. Biological evaluation has been performed using MC3T3-E1 pre-osteoblastic cells, conducting measurements on cell viability by means of the PrestoBlue® assay and cell morphology by Scanning Electron Microscopy (SEM). Osteogenesis related markers have been evaluated including the alkaline phosphatase (ALP) activity following a staining protocol and observation under a confocal laser fluorescence microscope. Collagen and calcium production by the cells have been determined by the O-cresol phthalein complexone (CPC) method and Sirius red staining, respectively. Calcium and phosphorous have been analyzed by Energy Dispersive Spectroscopy (EDS) and atomic-resolution mapping and biomineralization via X-Ray Diffraction (XRD). The mechanical stimulation on the cell-loaded constructs by applying uniaxial compression (by means of a MechanoCulture bioreactor) was based on a previous protocol [4] using 1 Hz frequency, 10% strain for a duration of 1 h every second day.

Physicochemical evaluation of the scaffolds

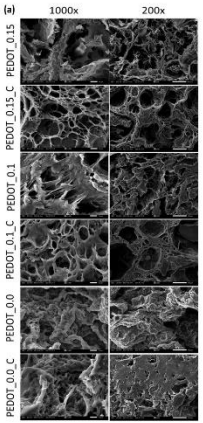

Figure 2. The porosity of all scaffold compositions depicted via SEM (a). Evaluation of % porosity calculated through ImageJ (b). Crosslinked scaffolds present higher porosity values than the non-crosslinked with the exception of the PVA-Gel (control) scaffolds, which exhibit fewer pores. PEDOT_0.15_C indicates the most well-defined pores.

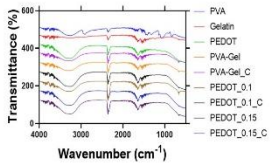

Figure 3. FTIR spectra of the different scaffold types and their basic components, PVA, gelatin, PEDOT:PSS. 'C' designates crosslinked scaffolds.

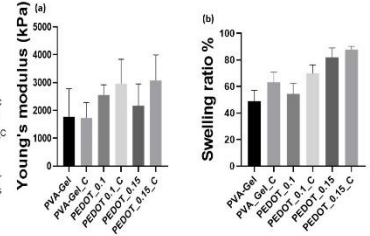

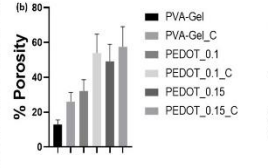

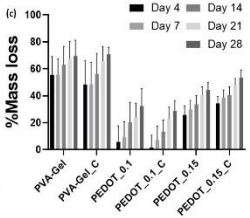

Figure 4. Evaluation of elastic modulus of the scaffolds at 60-95% strain, at the velocity of 15 mm/sec. PEDOT/PVA/Gelatin scaffolds presented favorable mechanical properties for bone tissue engineering. Their elastic modulus ranged between 1 and 5 MPa (a). Swelling ratios of the lyophilized scaffolds after 3 h immersion in PBS (b), and their respective degradation rates (c). The presence of PEDOT led to a significant increase of swelling ratio from 49% to 87% and a reduction of degradation rates from 75% to 50%.

Biological evaluation of the scaffolds

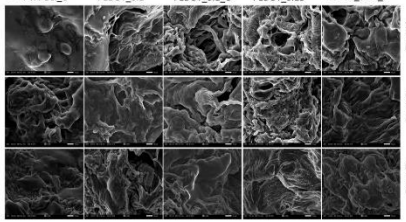

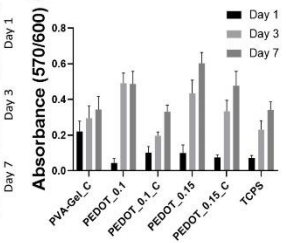

Figure 5. Representative SEM images showing the morphology of pre-osteoblastic cells seeded onto the different scaffold compositions after 1, 3 and 7 days. At day 3, a moderate cell number is visibly adhered onto the scaffolds, with the exception of PVA-Gel (control) scaffold, which exhibit fewer attached cells. At day 7, pre-osteoblasts have fully covered the surface of the scaffolds. Scale bar represents 10 μm (a). Cytotoxicity assessment on days 1, 3 and 7 expressed as absorbance values. All scaffolds exhibit great biocompatibility, with the PEDOT_0.15 slightly exceeding the other compositions (b).

Osteogenic differentiation in dynamic vs static cell culture

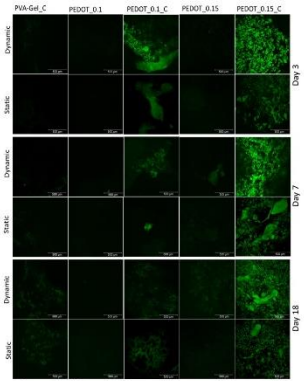

Figure 6. Alkaline phosphatase activity on days 3, 7 and 18 observed by confocal laser scanning microscopy following staining (green).

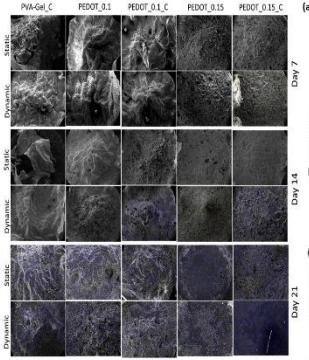

Figure 7. Determination of the calcium mineralization through atomic-resolution mapping and EDS analysis. Calcium is shown in yellow and phosphorous in purple dots.

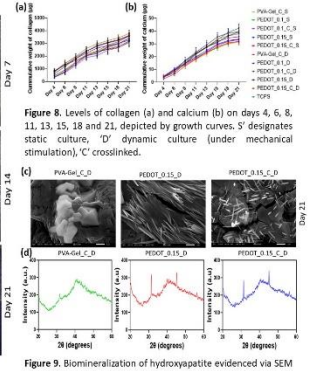

Figure 8. Levels of collagen (a) and calcium (b) on days 4, 6, 8, 11, 13, 15, 18 and 21, depicted by growth curves. 'S' designates static culture, 'D' dynamic culture (under mechanical stimulation), 'C' crosslinked.

Figure 9. Biomineralization of hydroxyapatite evidenced via SEM (c) and XRD analysis (d). 'S' designates static culture, 'D' dynamic culture (under mechanical stimulation), 'C' crosslinked.

Conclusion

The development of a self-triggered mechano-active scaffolds promote bone tissue regeneration based on our hypothesis. The results indicate that the PEDOT:PSS/PVA/Gelatin scaffolds support the adhesion, proliferation, and osteogenic differentiation of the pre-osteoblastic cells under mechanical stimulation. Particularly, the constructs of PEDOT_0.15 loaded scaffolds under mechanical stimulation enhanced biomineralization by the production of hydroxyapatite as evidenced via EDS and XRD analysis. The scaffolds demonstrate superior biological properties for bone tissue engineering and other load-bearing tissues with amplified matrix production via mechanical stimulation.

References

1. Florencio-Silva, R., et al., Biomed Res Int, **2015**
2. Guex, A.G., et al., Acta Biomater, **2017**
3. Schreivogel, S., et al., Journal of J Tissue Eng Regen Med, **2019**
4. Kontogianni et al, Bioengineering, **2023**

Acknowledgements

The research work was supported by the Hellenic Foundation for Research and Innovation (H.F.R.I.) under the "First Call for H.F.R.I. Research Projects to support Faculty members and Researchers and the procurement of high-cost research equipment grant" Project Number: HFRI-FM17-1999.

ID p12

NANOBODY-MEDIATED INHIBITION OF T-CELL ACTIVATION; BINDING SPECIFICITY STUDIES

P. Christou[1†], I. Tyritidis[1†], N. Koutras[1], K. Konnaris[1], K. Nika[1]

[1]Department of Biochemistry, School of Medicine, University of Patras, Patras, Greece; [†]These authors contributed equally to this work.

Introduction

The abnormal and undesirable overactivation of T-cells is a main characteristic for many pathological conditions, such as autoimmune diseases (1), as well as a side effect for T-cell-based immunotherapies, such as CAR-T-cell therapies (2). Therefore, many research strategies focus on manipulating the T-cell activation by **targeting the Lck protein**, a member of the Src family of protein tyrosine kinases (SFKs) (3). Lck is a **key protein for T-cells**, as it is responsible for the initiation of T-cell signaling after T-cell receptor (TCR) stimulation, making it an attractive target for inhibitory molecules (4). However, its high homology in the catalytic center with other SFK members (Lyn, Fyn, Src etc.) has been a barrier for its specific and efficient inhibition (5). The current study aims to the selective inhibition of Lck, by the intracellular expression of **blocking nanobodies (Nbs),** some small, camelid-derived antibody fragments. Here we experimentally assess the specificity of Nbs binding to Lck compared to other SFK members.

Materials and methods

Our laboratory has generated 30 different Nbs that recognize a poorly conserved region of Lck and has cloned them into plasmids for inducible eukaryotic expression. These Nbs were screened for Lck-binding after co-transfection with Lck in HEK293T cells. The top Nb candidate was then transduced in the Jurkat T-cell line for further testing of Nb's ability to bind the endogenous Lck. The same Nb was co-transfected with other SFKs in HEK293T cell lines and transduced in a B-cell line (BJAB) to test its binding to other SFKs. The binding ability was tested with co-immunoprecipitation (co-IP) assays and Western blots. Finally, confocal microscopy was used for the detection of colocalization. The Nbs were fused with an HA-tag in their C-terminus, in order to be detectable.

Results

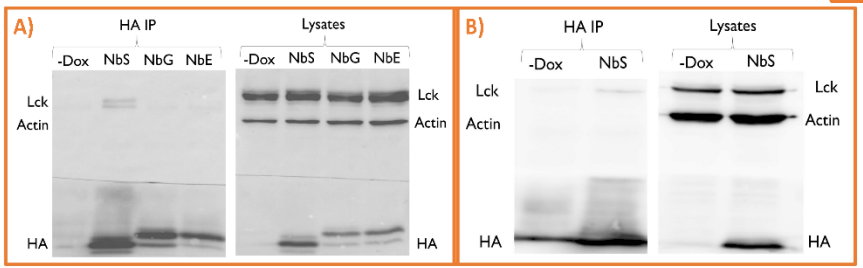

Figure 1. **NbS can bind to Lck intracellularly**.
Co-immunoprecipitation (co-IP) experiments for Lck and Nbs. Nbs were immunoprecipitated with anti-HA Ab and the bound Lck was detected by anti-Lck Western blot. The presence of Lck indicates a binding complex with Nb. Levels of Lck, Nb expression and actin in total lysates are shown at the right side of each co-IP.
A) Representative image during the screening of 30 different Nbs, showing at least one Nb (**NbS**) that has the ability to bind Lck.
B) Lenti-virally transduced Jurkat stable cell lines with **NbS** proved the intracellular binding with Lck in a T-cell environment.

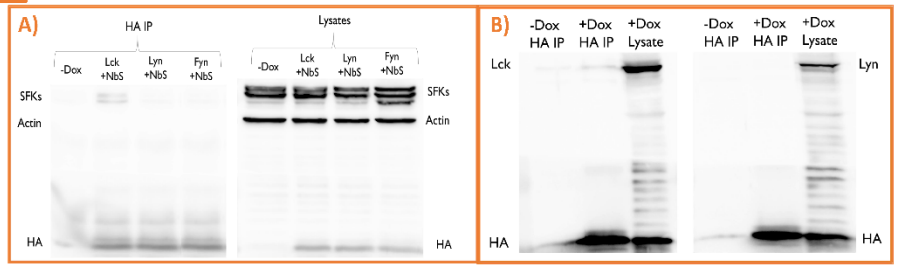

Figure 2. **NbS binds specifically to Lck but not to other SFKs.**
Co-immunoprecipitation (co-IP) experiments showing the specificity of **NbS**. **NbS** was immunoprecipitated with anti-HA Ab and the bound SFKs were detected with Western blot, using corresponding Abs. Levels of SFKs, Nb expression and actin in total lysates are shown at the right side of image.
A) HEK293T cells were double transfected with **NbS** and Lck, Lyn or Fyn, showing the specificity for Lck.
B) T-cell and B-cell lines were both transduced with **NbS** for the comparison of the binding with endogenous SFKs Lck and Lyn, respectively. Co-IP shows binding only to Lck.

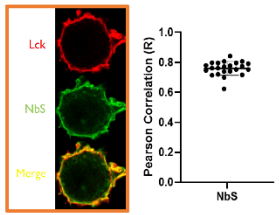

Figure 3. **NbS and Lck colocalize at the plasma membrane.**
Left) Stable Jurkat lines expressing **NbS** were stained with anti-Lck (red) and anti-HA (green) and analyzed by confocal microscopy. Yellow shows colocalization.
Right) Collective data of colocalization analysis (R coefficient) from N=23 cells are shown in the adjacent graph.
R=0 no colocalization, R=1 perfect colocalization

Conclusions

1) The top Nb candidate **NbS** was capable of binding both exogenously expressed Lck in HEK293T cells and endogenous Lck in T cells, intracellularly.
2) **NbS** shows specificity to only bind Lck and not other SFKs, either exogenously expressed (Lyn, Fyn) or endogenous (Lyn).
3) **NbS** and Lck show strong colocalization at the plasma membrane, the natural compartment of Lck localization.
4) Functional studies need to be done in order to reveal the possible downstream effects of the **NbS**-Lck binding.

References

1. Malmström, V., Trollmo, C., & Klareskog, L. (2005). Modulating co-simulation: A rational strategy in the treatment of rheumatoid arthritis. In *Arthritis Research and Therapy* (Vol. 7, Issue SUPPL. 2).
2. Siegler, E. L., & Kenderian, S. S. (2020). Neurotoxicity and Cytokine Release Syndrome After Chimeric Antigen Receptor T Cell Therapy: Insights Into Mechanisms and Novel Therapies. In *Frontiers in Immunology* (Vol. 11). Frontiers Media S.A.
3. Rossy, J., Williamson, D. J., & Gaus, K. (2012). How does the kinase Lck phosphorylate the T cell receptor? Spatial organization as a regulatory mechanism. In *Frontiers in Immunology* (Vol. 3, Issue JUN).
4. Lee, K. C., Ouwehand, I., Giannini, A. L., Thomas, N. S., Dibb, N. J., & Bijlmakers, M. J. (2010). Lck is a key target of imatinib and dasatinib in T-cell activation. In *Leukemia* (Vol. 24, Issue 4, pp. 896–900). Nature Publishing Group.
5. Engen JR, Wales TE, Hochrein JM, Meyn MA, Banu Ozkan S, Bahar I, et al. Structure and dynamic regulation of Src-family kinases. Cell Mol Life Sci. 2008;65:3058–73.

Acknowledgement: This research has been co-financed by the European Union and Greek national funds through the Operational Program Competitiveness, Entrepreneurship and Innovation, under the call RESEARCH – CREATE – INNOVATE

Co-financed by Greece and the European Union

Epigenetic silencing of the glucocorticoid receptor to broaden the applicability of antigen-specific T-cell immunotherapy

M. Alvanou[1,2], P. Selidis[1,3], P. Christophi[1,2], P. Simonopoulos, M. Yiangou[3], I. Sakellari[1], A. Spyridonidis[2], N. Psatha[3], E. Yannaki[1,4] A. Papadopoulou[1]

[1]Gene and Cell Therapy Center, George Papanikolaou Hospital, Thessaloniki, Greece, [2]School of Medicine, University of Patras, Patras, Greece, [3]Department of Genetics, Development and Molecular Biology, School of Biology, Aristotle University of Thessaloniki, Thessaloniki Greece, [4]University of Washington, Seattle, United States

BACKGROUND/AIM

Viral and fungal infections are among the most fatal complications in patients undergoing allogeneic hematopoietic stem cell transplantation (allo-HSCT). Adoptive immunotherapy (AI) with pathogen-specific T cells (pSTs) represents an attractive alternative therapy for opportunistic infections after allo-HSCT. However, T cells perform suboptimally under immunosuppression, mainly steroids, which represent the first-line treatment of transplant-associated immunological complications. The latter generates the obvious paradox of depriving the most susceptible to infections patients of the potential benefits of AI and the need to improve current T-cell AI. We have recently reported the generation of steroid-resistant pSTs, by genetic disruption of the glucocorticoid receptor (GR) gene (NR3C1) using CRISPR/Cas9 editing. To minimize the possibility of unpredictable genomic changes by gene editing, we here, aimed to investigate whether GR-resistant cells could be developed by precision epigenome editing.

METHODS

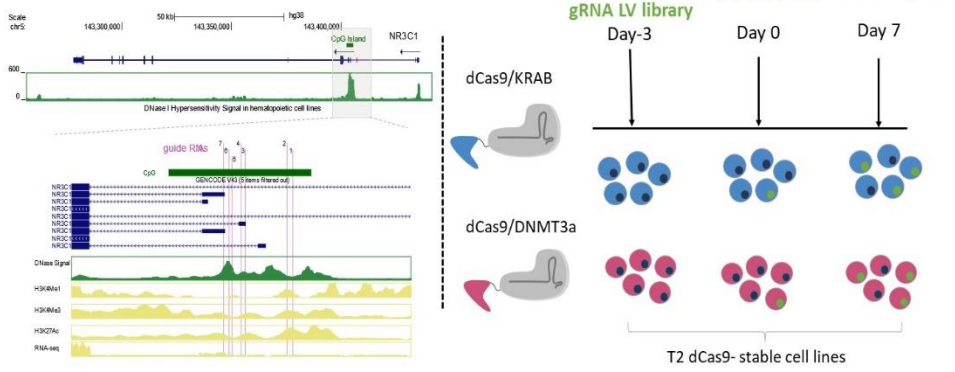

RESULTS

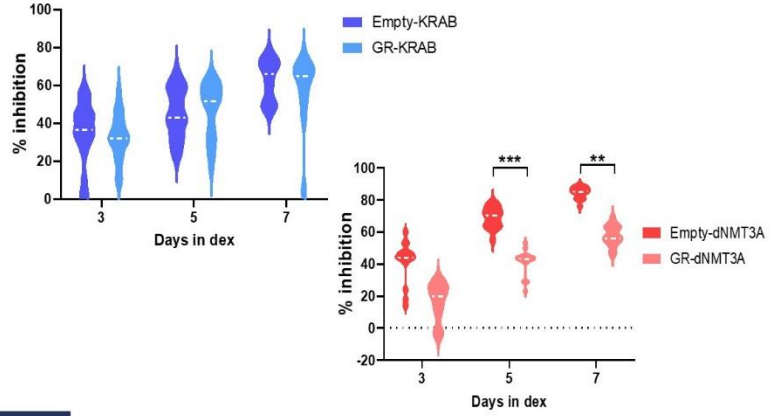

CONCLUSIONS

Overall, we present a proof-of-concept, feasibility study of epigenetically disrupting the expression of GR by a DNA methyltransferase to selectively confer resistance to steroids. Further studies on screening additional gRNAs and transcriptional repressors or multiplex targeting towards GR inactivation are in process, so as to identify an optimized epi-editing tool to be subsequently tested in primary T cells.

Acknowledgement: Funding for this project was provided in part by the State Scholarships Foundation (I.K.Y.).

ID p14

Identification of novel γ-globin repressors through a custom CRISPR knockout screen and validation studies for the treatment of β-haemoglobinopathies

Sevgi Özkaramehmet, Anthi Demetriadou, Petros Patsali, Maria Xenophontos, Carsten W. Lederer, Coralea Stephanou, Petros Kountouris, Marios Phylactides, Marina Kleanthous

Molecular Genetics Thalassemia Department, The Cyprus Institute of Neurology and Genetics, P.O. Box 23462, 1683 Nicosia, Cyprus

INTRODUCTION

Haemoglobinopathies are a group of conditions affecting haemoglobin. The haemoglobin tetramer consists of two α- and two β-globin chains ($\alpha_2\beta_2$). Mutations in the *HBB* gene, which encodes for the β-globin chain, cause two of the most common inherited monogenic disorders, **β-thalassaemia and sickle cell disease**. Cyprus has the third highest percentage (12%) of β-thalassaemia carriers.

Reactivation of the *γ-globin* gene for the production of fetal haemoglobin (HbF) is a promising therapeutic strategy. Pharmacological targeting of BCL11A and LRF (*ZBTB7A*), the main transcription factors regulating γ-globin levels, is difficult and complicated , especially since they are also involved in the regulation of multiple non-erythroid genes. Thus, **identification of new factors amenable to pharmacologic control for the treatment of β-haemoglobinopathies is of utmost importance**

AIMS OF THE STUDY

- To perform a custom CRISPR/Cas9 knockout screen for a set of 293 selected genes for the discovery of novel γ-globin repressors which can be potential druggable targets for the treatment of β-haemoglobinopathies.
- To validate the candidate genes for the screening phenotype (HbF upregulation) in HUDEP-2 cells.

MATERIALS & METHODS

Experimental workflow of the CRISPR knockout screen and validation of the candidate genes

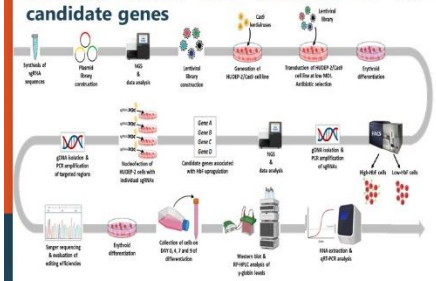

RESULTS

1. Generation of the sgRNA library targeting the genes of interest

- Genes were selected from previously published data (IthaGenes database and from published studies).
- 1250 sgRNAs
  - 293 candidate genes
  - 8 positive control genes
  - 46 non-targeting control sgRNAs

  } 4 sgRNAs/gene
- The sgRNA sequences were retrieved from the Brunello human genome-wide CRISPR library.

2. Generation of a HUDEP-2 cell line stably expressing an active form of the Cas9 endonuclease

- Transduction of the HUDEP-2 cell line with Cas9-lentiviruses (lentiCas9-Blast LV) at a MOI=0.3.
- The expression and activity of Cas9 protein were evaluated via **western blot (A)** and a **flow cytometry-based assay (B)**, respectively.

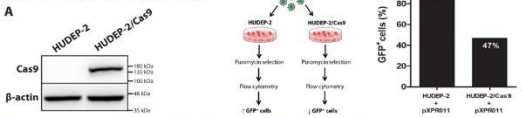

Figure 1. HUDEP-2/Cas9 cell line expresses an active form of the Cas9 endonuclease

A. Protein extracts from HUDEP-2 and HUDEP-2/Cas9 cell lines were subjected to western blot using an antibody against Cas9. An antibody that recognizes β-actin was used as a loading control.

B. Left: Schematic of the experimental procedure followed for the evaluation of the Cas9 activity. Right: Bar chart showing the percentage of GFP⁺ cells following flow cytometry analysis of HUDEP-2 or HUDEP-2/Cas9 cell lines transduced with the pXPR-011 lentiviruses (deliver both the GFP coding sequence and a sgRNA targeting GFP). A reduction of 47% in GFP⁺ cells was observed in HUDEP-2/Cas9 cell line, as compared to HUDEP-2 cells.

3. Transduction of the HUDEP-2/Cas9 cell line with the lentiviral library

- HUDEP-2/Cas9 cell line was transduced with the lentiviral library at a low MOI (0.1-0.4) in order to ensure that most cells will receive only one sgRNA.
- Transduction was scaled up accordingly in order for a representation of ~500x to be achieved.
- Following antibiotic selection (puromycin treatment) to remove all the untransduced cells, erythroid cell differentiation was induced for a total of seven days.

4. FACS-based screening selection

- Cells at DAY7 of differentiation were stained for HbF and sorted in HbF-high and HbF-low cell populations using the BD FACSAria™ III Cell Sorter.

Figure 2. FACS-based separation of HbF-high and HbF-low expressing cells

Representative HbF FACS gating strategy for sorting the HbF-high & HbF-low cell populations.

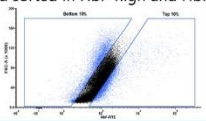

RESULTS

5. Analysis of the screen to identify candidate genes associated with HbF upregulation

- The sgRNAs targeting Gene A, Gene B and Gene C were significantly enriched in the HbF-high population, suggesting that they might act as γ-globin repressors.
- **Gene A** encodes for a protein involved in ion transport and iron homeostasis.
- **Gene B** is a transcriptional regulator.
- **Gene C** plays a central role in chromatin remodelling and acts as a transcription regulator.

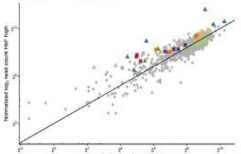

Figure 3. Screening results

Scatter plot of HbF-high (Y-axis) and HbF-low (X-axis) populations as $\log_2$ transformed normalized read counts. Each dot represents a sgRNA. Data show the average normalized read counts from four biological replicates ($n=4$).

6. Nucleofection of HUDEP-2 cells with individual sgRNAs and evaluation of editing efficiencies

- HUDEP-2 cells were either transduced with lentiviral vectors or nucleofected individually with four synthetic sgRNAs for Gene A, B and C.
- The editing efficiencies of sgRNAs were evaluated with ICE analysis by Synthego after Sanger sequencing.
- The editing efficiencies of the sgRNAs ranged between 85-90%.

7. Analysis of γ-globin levels

- HUDEP-2 cells were collected on Days 0, 7 and 9 of differentiation for analysing levels of γ-globin via western blot and RP-HPLC.
- The editing efficiencies observed at the DNA level does not translate to the protein level for Gene A and Gene B.
- The knockdown of Gene C was confirmed by western blot for three out of four sgRNAs.

FUTURE WORK

- The mechanism of action of the candidate genes will be investigated with regards to erythroid maturation and haemoglobin switching.
- The discrepancies between DNA editing efficiencies and protein levels will be investigated.

CONTACT

Dr. Marios Phylactides
(mphylact@cing.ac.cy)

The project EXCELLENCE/1216/0389 is co-funded by the European Regional Development Fund and the Republic of Cyprus through the Research and Innovation Foundation.

ID p15

p15

HELLENIC PASTEUR INSTITUTE

Mechanisms of αSynuclein-mediated coordination of RNA metabolism

P. Chandris[1], K. Segklia[1], M. Samiotaki[2], N. Antoniou[1], G. Panayotou[2], R. Matsas[1], E. Taoufik[1]

1: Laboratory of Cellular, Molecular Neurobiology and Stem Cell Biology, Hellenic Pasteur Institute, 11521 Athens, Greece
2: BSRC Alexander Fleming, Vari, 11364, Attiki, Greece

Abstract

Parkinson's disease (PD) is a severe neurodegenerative disorder. The disease is linked to the aggregation of a small amyloid protein, alpha synuclein (aSyn), whish is implicated in synaptic vesicle trafficking and neurotransmitter release. In PD, aSyn is found in brain inclusions. A well characterized mutation of aSyn (G209), encodes for A53T protein which is directly linked to the familial type of PD. In this study, we use a toolikit of neuronal cell line stably exrpessing A53T aSyn, primary hipoccampal neurons from A53T transgenic mice and patient derived hiPSC-neurons. Our proteomic analysis of hiPSC neurons links aSyn A53T mutation to altered expression levels of molecules involved in RNA metabolism. Combining -"omics" approaches with live cell imaging, SR microscopy and smFISH, we aim in investigating how the expression of aSyn A53T affects RNA dynamics in neurons. Our initial data bridge aSyn biology to RNA granule formation with an imbalanced metabolism of RNA machinery triggered by the presence of A53T aSyn in cellular models of PD.

Introduction

1

- PD is the 2nd most common ND disease
- There is idiopathic and familial PD
- PD exhibits motor and non-motor deficits
- aSyn is found in Lewy Bodies
- aSyn A53T is directly linked to familial PD

Results

2 Transgenic mice for human A53T aSyn develop PD escorted by aSyn inclusions in Lewy Bodies

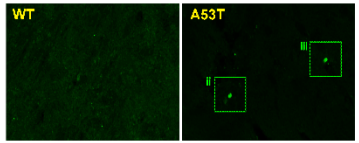

Mouse A53T model (M83; B6;C3-Tg(Prnp-SNCA*A53T)83Vle/J Giasson et al, 2002)

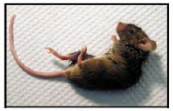

3 Elevation of RNA metabolism and protein synthesis machinery proteins in A53T iPSC neurons

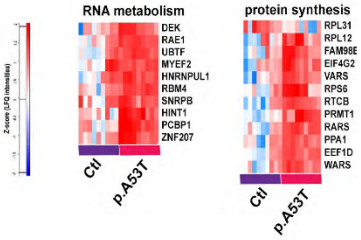

4 SHSY-5 neuroblastoma cells expressing aSyn A53T exhibit reduced response to arsenite stress and eIF2a phosphorylation

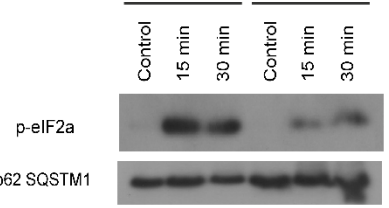

5 Live cell imaging in cells expressing the pathogenic aSyn (A53T) reveals a delayed cellular response in Stress Granule formation upon arsenite treatment

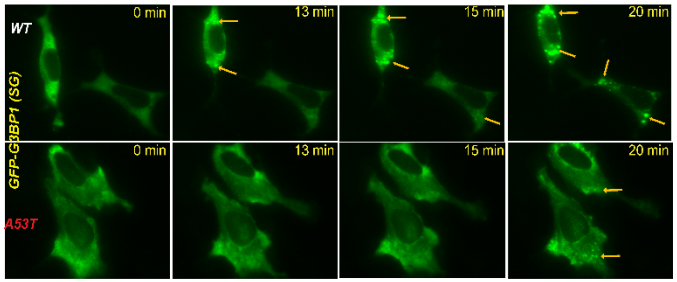

6 Super resolution unveills sequestration of aSyn in RNA granule subdomains

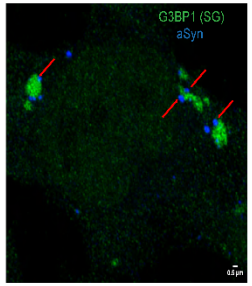

7 aSyn smFISH and cluster analysis unveils sequestration of RNA in the soma of A53T hippocampal mouse neurons

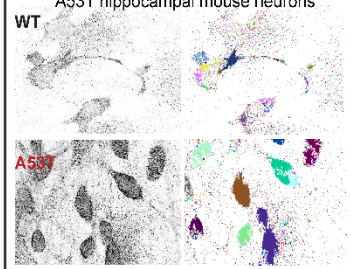

Perspectives - Ongoing Experiments

- Dissecting the role of aSyn fibrillation in RNA granule machinery
- Investigating dynamics of aSyn mRNA and potential interactions with RBPs
- Tool-building for live cell single molecule RNA imaging

Acknowledgments: Funded by H.F.R.I. (ProjectNumber: 1019; to RM) and by EPANEK-ESPA Program (Project Number: T2ΕΔΚ-02813 & MIS 5131418: to RM)

Related literature

Giasson et. al. Neuron 2002 May 16;34(4):521-33
Antoniou et. al. NPJ Parkinsons Dis. 2022 Feb 11;8(1):15.
Hallachli et. al. Cell 2022 Vol. 185, Issue 12, pp. 2035-2056

ID p16

MICROGLIAL SIGNATURES IN AN IN VIVO FAMILIAL PARKINSON'S DISEASE MODEL

E. Ninou[1], G. Zejneli[2], K. Segklia[1], K. Charmpi[1], P. Handris[1], O. Mirabeau[2], A. Deczkowska[2], E. Taoufik[1]

[1] Laboratory of Cellular and Molecular Neurobiology-Stem Cells, Hellenic Pasteur Institute, 11521 Athens, Greece, [2] Brain-Immune Communication Lab, Institut Pasteur, Université Paris Cité, Inserm U1224, F-75015, Paris, France.

Parkinson's disease (PD) is the second most common neurodegenerative (ND) disorder presenting a wide range of manifestations. Despite extensive research, the pathophysiology of PD is still unknown, and the lack of therapeutic options presents a huge clinical unmet need. A common denominator of most ND disorders is synaptic dysfunction that is caused by changes in synaptic structure and function, which can be either the cause or the effect of the disease etiology. Recent data in neuropsychiatric disorders suggest a neurodevelopmental origin for synaptic dysfunction which contrasts with a decades-long axiom, that synaptic dysfunction is among the end-results of ND. This contradicting theory was recently supported by the discovery of unexpected commonalities in the operating mechanisms in both developmental and ND conditions. These findings suggest that synaptic dysregulation is the result of improper glial-neuronal interactions, not only in adulthood, but as early as critical embryonic and postnatal developmental time-points for the neuronal circuits, where the importance of microglia is well established. Understanding the role of microglia early in ND can improve our understanding and open a path for new therapeutic targets. Our study utilizes single-cell-level techniques in the familial PD αSyn A53T model to shed light on the role of microglial-neuronal interactions during the pre-symptomatic stages of PD development and disease progression. Using this non-neurocentric approach, we will characterize the involvement of microglia on PD progression, disease-related subpopulations, and potential therapeutic disease modifying targets in PD.

Transgenic mice for human A53T aSyn develop PD escorted by aSyn inclusions in Lewy Bodies

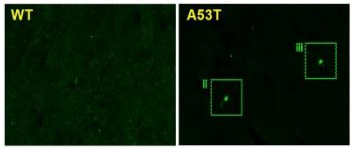

Mouse A53T model (M83; B6;C3-Tg(Prnp-SNCA*A53T)83Vle/J Giasson et al, 2002)

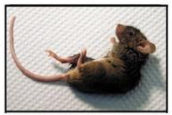

Sorting pipeline of M83 and control microglia cells

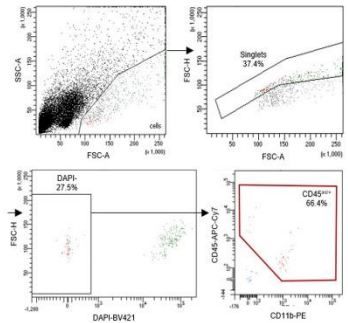

MARS-seq2.0

Immunocytochemical characterization of M83 and control cortical microglia cells shows differences in number of cells and circularity already at P7

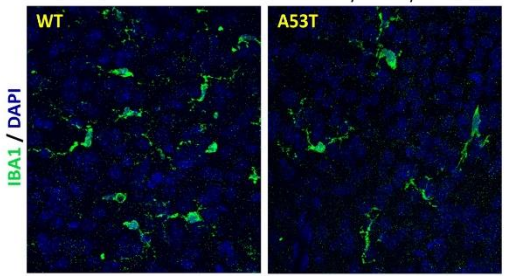

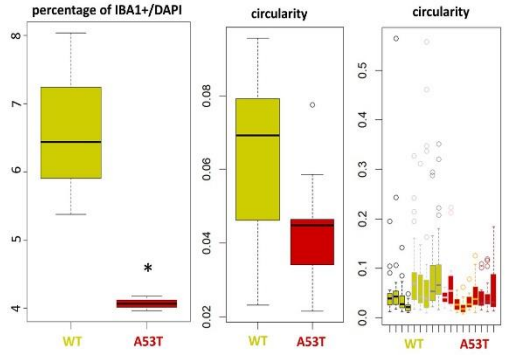

αSyn clusters within IBA-1+ cells at P7, P30, P90

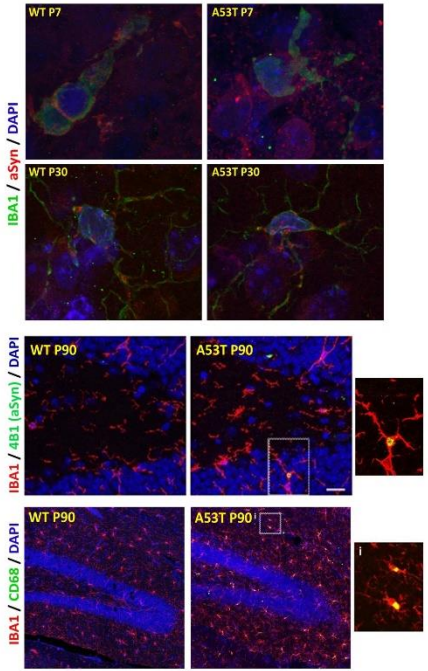

scRNA-seq in microglia from M83 transgenic mice and wild-type control littermates brains to **identify how the neuronal pA53T-αSyn expression alters microglia subpopulations** and PD associated signaling pathways, prior to symptoms onset

extensive **immunocytochemical characterization** of microglia in multiple regions of M83 mice to **identify the effects of neuronal pA53T-αSyn on microglia** during the early brain developmental stages and disease progression

findings from scRNA seq analyses are validated by analysis of the **spatiotemporal pattern of selected αSyn affected microglia-associated molecules**, using **smRNA-FISH** and **immunodetection** in M83 mice

Acknowledgements: Funded by the Hellenic Foundation for Research and Innovation (H.F.R.I.) under the "1st Call for H.F.R.I. Research Projects to support Faculty members and Researchers and the procurement of high-cost research equipment" (Project Number: 1019; to RM); Hellenic Pasteur Institute post-doctoral fellowship awarded to EN

ID p17

PARACRINE EFFECTS OF ASTROCYTES IN PARKINSON'S DISEASE PATHOLOGY: A STUDY USING IPSC-DERIVED NEURONS AND ASTROCYTES CARRYING THE P.A53T-ASYN MUTATION

S. Dede[1], O. Apokotou[1], A. Kollias[2], C.Paschou[2], E. Taoufik[2], R. Matsas[2], F. Papastefanaki[1, 2]

1.Human Embryonic and Induced Pluripotent Stem Cell Unit, Hellenic Pasteur Institute, Athens, Greece

2.Laboratory of Cellular and Molecular Neurobiology-Stem Cells, Hellenic Pasteur Institute, Athens, Greece

ΕΛΛΗΝΙΚΟ ΙΝΣΤΙΤΟΥΤΟ ΠΑΣΤΕΡ
INSTITUT PASTEUR HELLENIQUE

Introduction

Synucleinopathies are a group of neurodegenerative disorders characterized by misfolded α-Synuclein (αSyn) aggregates in the central and peripheral nervous systems. In Parkinson's disease (PD) one of the best-researched mutations is G209A in the SNCA gene resulting in the pathological p.A53T-αSyn protein. While most research work had focused on neuron-intrinsic deficits and degeneration, studies introducing neuron-glia interactions in PD pathology have recently started emerging. Astrocytes, the most abundant cells in human brain, play critical roles in neuronal health while they can exert neuroprotective or neurotoxic effects upon disease. Recent studies demonstrate that astrocytes may contribute to neuronal health status through their secretome(1,2). **Our aim is to elucidate whether there are interactions between astrocytes and neurons carrying the p.A53T-αSyn mutation that are facilitated by secreted mediators and contribute to PD pathology.**

Materials & Methods

We used our previously established induced pluripotent stem cell (iPSC)-based neuronal model from patients harboring the p.A53T-αSyn mutation and additionally generated and characterized ventral midbrain-patterned iPSC-derived astrocytes. To investigate the paracrine mechanisms underlying the midbrain neuron-astrocyte interactions, both healthy and p.A53T neurons were treated with healthy and p.A53T astrocyte conditioned media (ACM) at all possible combinations.

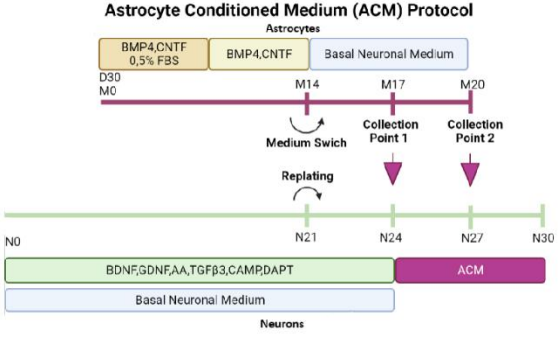

1 Healthy astrocyte conditioned medium ameliorates disease-associated phenotypes in PD neurons

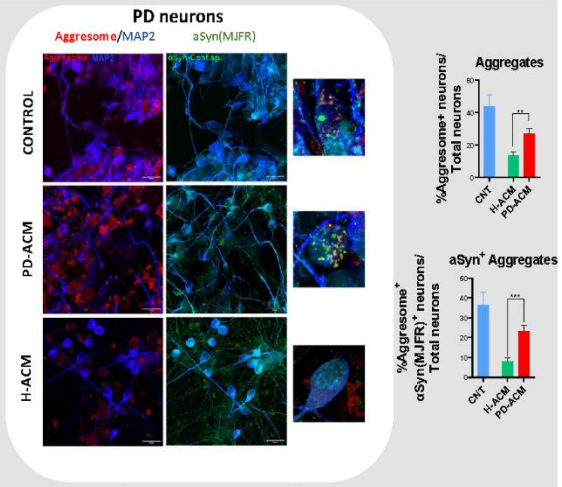

Treatment of p.A53T-αSyn neurons with conditioned medium from healthy astrocytes reduces the number of detected intraneuronal protein aggregates and aSyn aggregates.

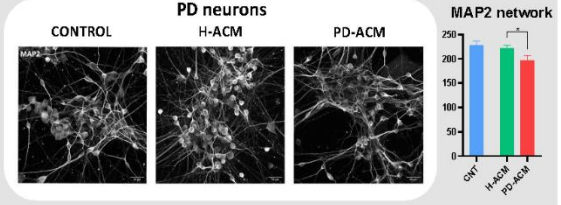

Treatment of p.A53T-αSyn neurons with conditioned medium from healthy astrocytes (healthy ACM vs PD ACM) ameliorates neurite network extension.

2 PD astrocyte conditioned medium affects viability of healthy neurons

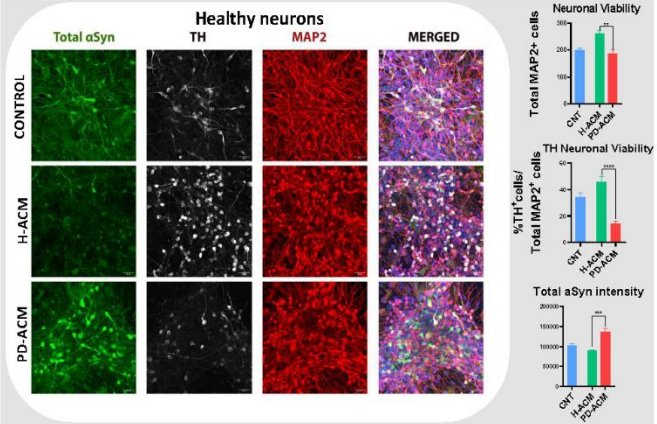

Healthy neurons treated with conditioned medium from p.A53T-αSyn astrocytes display reduced neuronal viability with an increased vulnerability of tyrosine hydroxylase-positive dopaminergic neurons, and increased levels of total neuronal aSyn.

Conclusions

Our results indicate that p.A53T-αSyn mutant astrocytes contribute to the neurodegeneration process whereas healthy astrocytes mitigate the pathological phenotype of PD neurons and that these effects are mediated at least partially through their secretome in a paracrine fashion. The study of the underlying molecular/cellular pathways is ongoing.

Funding

Supported by the Hellenic Foundation for Research and Innovation (H.F.R.I.) under the "1st Call for H.F.R.I. Research Projects to support Faculty members and Researchers and the procurement of high-cost research equipment" (Project 1019-DiseasePhenoTarget).

ΕΛΙΔΕΚ

References

1.Yang, Y., Song, J. J., Choi, Y. R., Kim, S. H., Seok, M. J., Wulansari, N., Darsono, W. H. W., Kwon, O. C., Chang, M. Y., Park, S. M., & Lee, S. H. (2022). Therapeutic functions of astrocytes to treat α-synuclein pathology in Parkinson's disease. *Proceedings of the National Academy of Sciences of the United States of America*, *119*(29), e2118746119. https://doi.org/10.1073/pnas.2118746119

2. Barbar, L., Jain, T., Zimmer, M., Kruglikov, I., Sadick, J. S., Wang, M., Kalpana, K., Rose, I. V. L., Burstein, S. R., Rusielewicz, T., Nijsure, M., Gutterplan, K. A., di Domenico, A., Croft, G., Zheng, B., Nabutu, H., Hebert, J. M., Liddelow, S. A., & Fossati, V. (2020). CD49f Is a Novel Marker of Functional and Reactive Human iPSC-Derived Astrocytes. *Neuron*, *107*(3), 436–453.e12. https://doi.org/10.1016/j.neuron.2020.05.014